Nordita program on "Computational Challenges in Nuclear and Many-Body Physics" , Sep. 15 - Oct. 10, 2014, Stockholm

Multi-Dimensionally Constrained Covariant Density Functional Theories: Formalism and Applications

Shan-Gui Zhou (周善贵)

Institute of Theoretical Physics,
Chinese Academy of Sciences, Beijing

Contents

- Introduction
- Multidimensionally-constrained CDFTs
- Normal nuclei
  - 1-, 2-, & 3-dim PES of ^{240}Pu & fission barriers of actinides
  - Non-axial octupole (tetrahedral) shapes in *N* = 150 isotones
  - Superdeformed & hyperdeformed shapes in actinides
- Λ hypernuclei
  - Shape polarization effect of Λ
  - Superdeformed shapes in Λ hypernuclei
- Summary & perspectives

Nuclear shapes

$$R(\theta,\varphi) = R_0\left[1 + \beta_{00} + \sum_{\lambda=1}^{\infty}\sum_{\mu=-\lambda}^{\lambda}\beta^*_{\lambda\mu}Y_{\lambda\mu}(\theta,\varphi)\right]$$

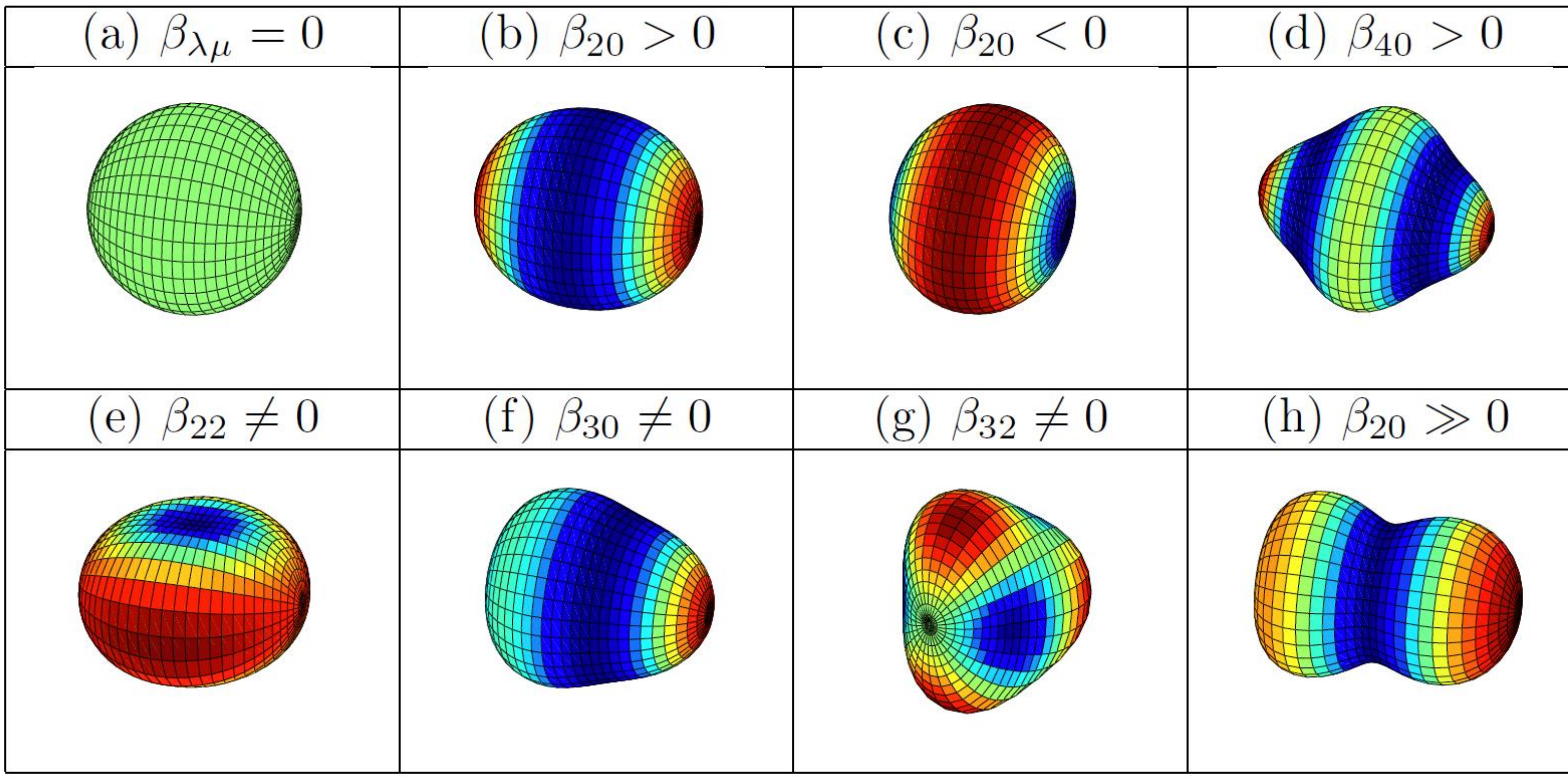

Courtesy of Bing-Nan Lu (吕炳楠)

Nonaxial quadrupole shape (β_{22} or γ)

Meng_Zhang 2010_JPG37-064025

J. Phys. G: Nucl. Part. Phys. **37** (2010) 064025

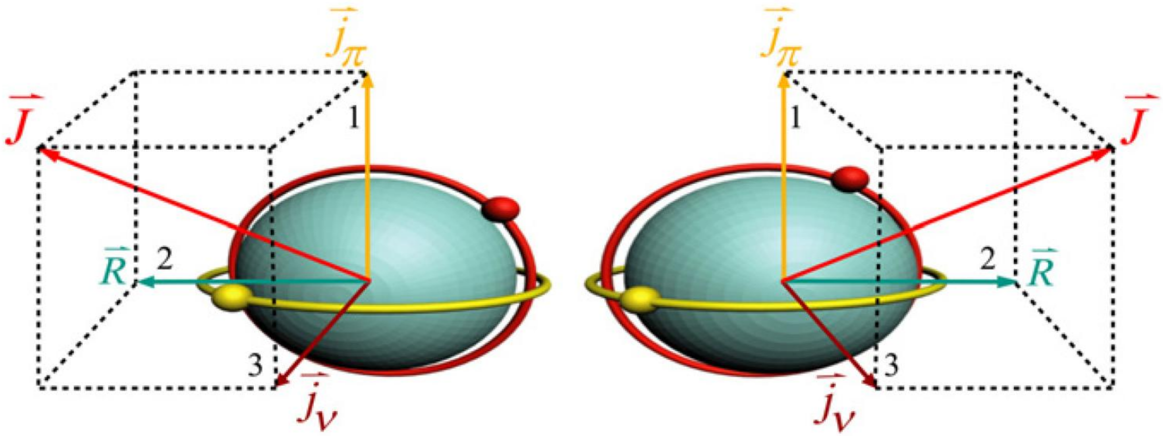

Figure 1. Left- and right-handed chiral systems for a triaxial odd–odd nucleus.

A static triaxial shape in atomic nuclei manifests itself by

the wobbling motion & chiral doublet bands

Bohr & Mottelson 1975
Odegard … 2001_PRL86-5866

Frauendorf_Meng1997_NPA617-131
Starosta … 2001_PRL86-971
…

Octupole shape (β_{30})

Gaffney… 2013_Nature497-199

ARTICLE

doi:10.1038/nature12073

Studies of pear-shaped nuclei using accelerated radioactive beams

L. P. Gaffney[1], P. A. Butler[1], M. Schec
N. Bree[7], J. Cederkäll[8], T. Chupp[9], D.
M. Huyse[7], D. G. Jenkins[13], D. T. Joss[1],
P. Napiorkowski[14], J. Pakarinen[4,12], M
S. Sambi[7], M. Seidlitz[5], B. Siebeck[5], T.
K. Wimmer[18], K. Wrzosek-Lipska[7,14]

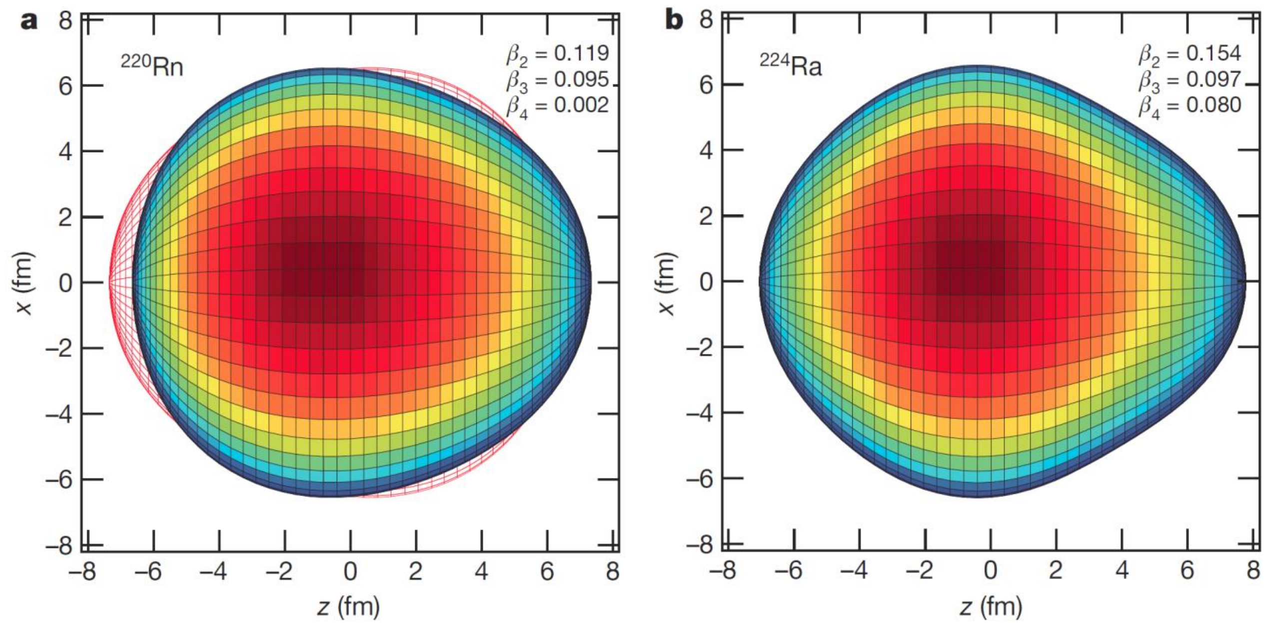

Nonaxial (β_{22} or γ) & octupole (β_{30}) shapes in PES

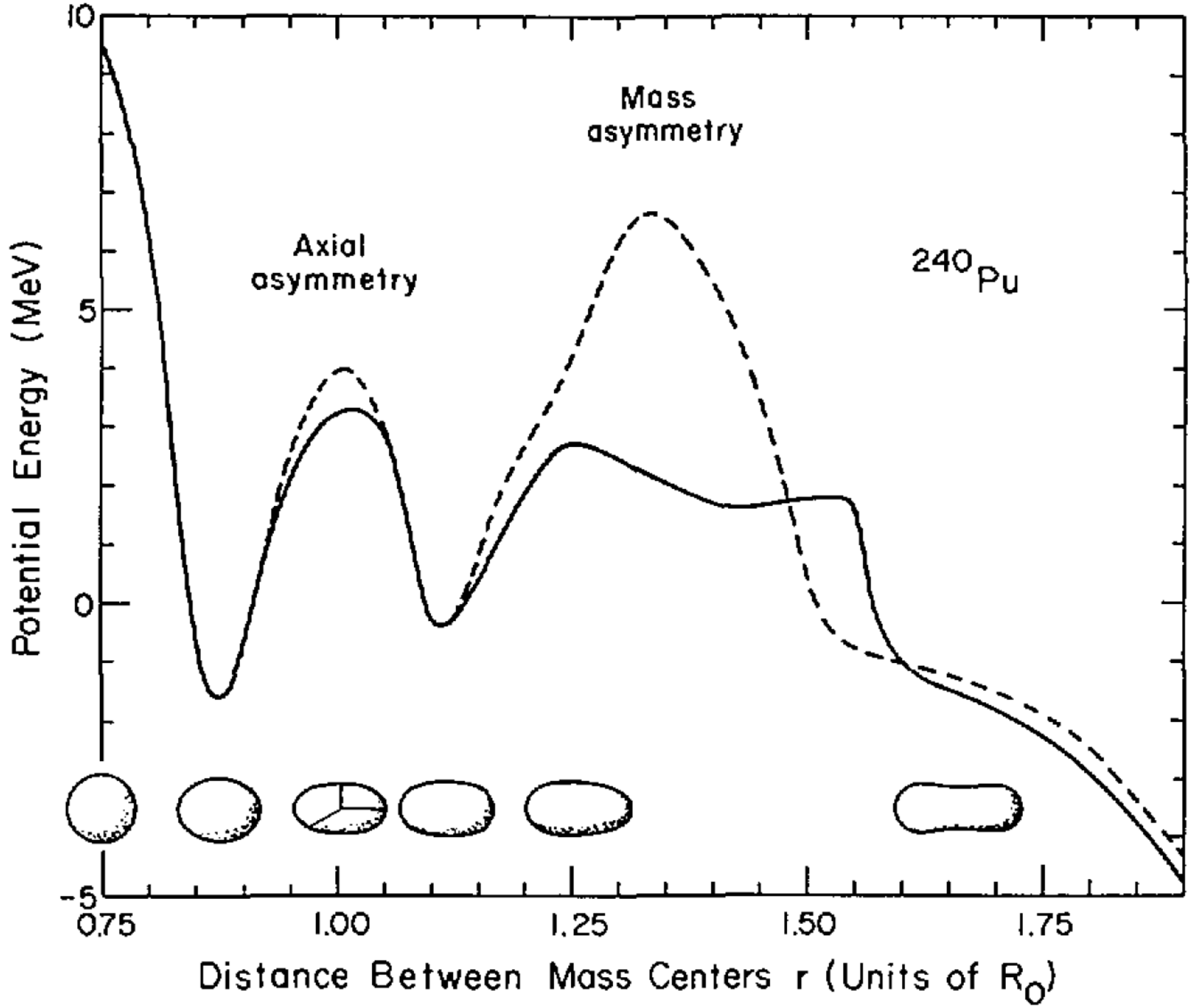

Möller_Nix 1973
IAEA-SM-174/202

Axial asymmetry plays important roles around the first barrier

Reflection asymmetry plays important roles around the second barrier

Nonaxial (β_{22} or γ) & octupole (β_{30}) shapes in PES

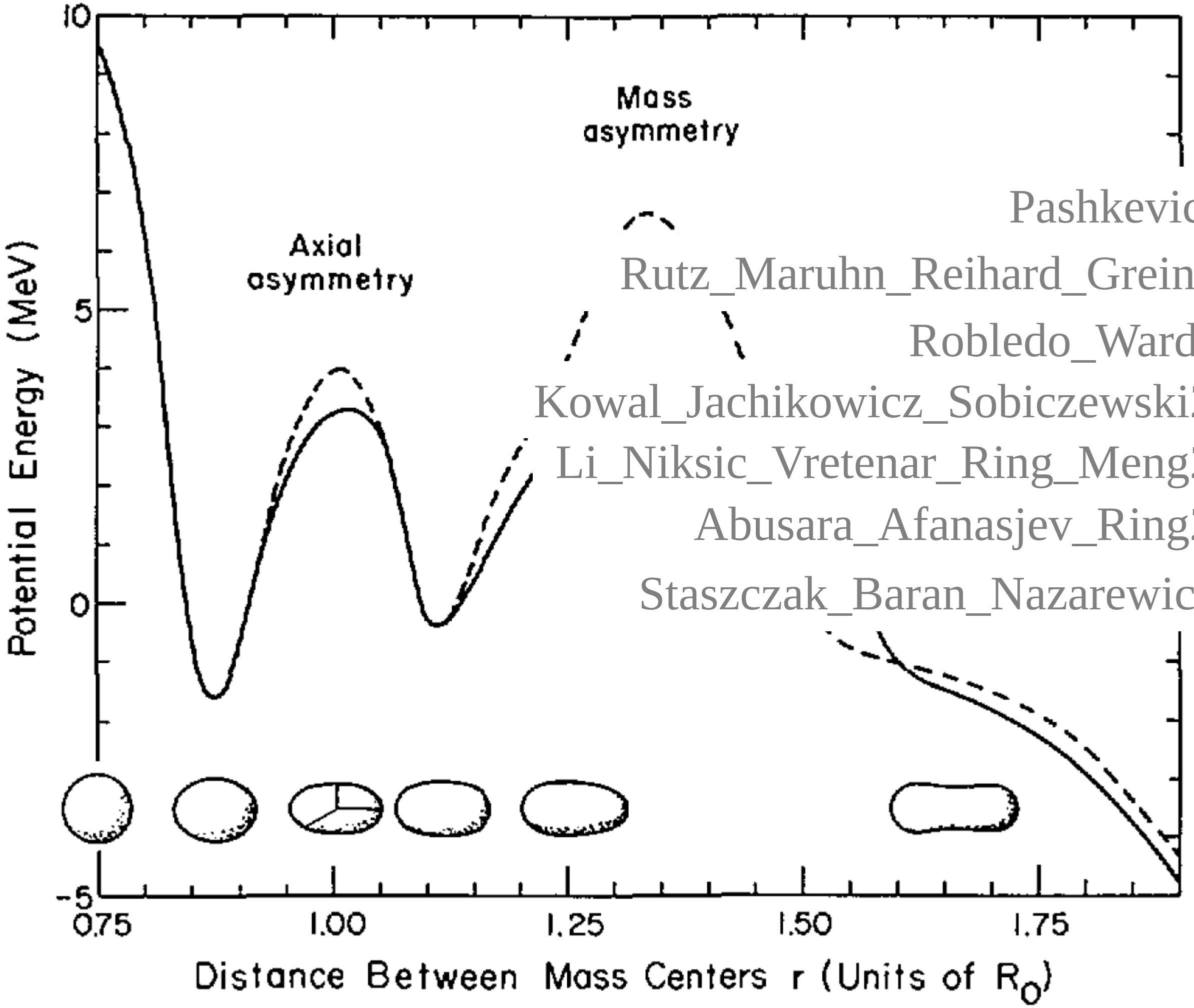

Möller_Nix 1973
IAEA-SM-174/202

Pashkevich1969_NPA133-400
Rutz_Maruhn_Reihard_Greiner1995_NPA590-680
Robledo_Warda2008_IJMPE17-204
Kowal_Jachikowicz_Sobiczewski2010_PRC82-014303
Li_Niksic_Vretenar_Ring_Meng2010_PRC81-064321
Abusara_Afanasjev_Ring2010_PRC82-044303
Staszczak_Baran_Nazarewicz2011_IJMPE20-552
…

Axial asymmetry plays important roles around the first barrier
Reflection asymmetry plays important roles around the second barrier

Covariant Density Functional Theory (CDFT)

$$\mathcal{L} = \bar{\psi}_i \left(i\partial\!\!\!/ - M \right) \psi_i + \frac{1}{2}\partial_\mu\sigma\partial^\mu\sigma - U(\sigma) - g_\sigma\bar{\psi}_i\sigma\psi_i$$
$$- \frac{1}{4}\Omega_{\mu\nu}\Omega^{\mu\nu} + \frac{1}{2}m_\omega^2\omega_\mu\omega^\mu - g_\omega\bar{\psi}_i\omega\!\!\!/\psi_i$$
$$- \frac{1}{4}\vec{R}_{\mu\nu}\vec{R}^{\mu\nu} + \frac{1}{2}m_\rho^2\vec{\rho}_\mu\vec{\rho}^\mu - g_\rho\bar{\psi}_i\vec{\rho\!\!\!/}\vec{\tau}\psi_i$$
$$- \frac{1}{4}F_{\mu\nu}F^{\mu\nu} - e\bar{\psi}_i\frac{1-\tau_3}{2}A\!\!\!/\psi_i,$$

Serot_Walecka1986_ANP16-1

Reinhard1989_RPP52-439

Ring1996_PPNP37-193

Vretenar_Afanasjev_Lalazissis_Ring2005_PR409-101

Meng_Toki_SGZ_Zhang_Long_Geng2006_PPNP57-470

$$\left(\boldsymbol{\alpha}\cdot\mathbf{p} + \beta(M + S(\mathbf{r})) + V(\mathbf{r})\right)\psi_i = \epsilon_i\psi_i$$

$$\left(-\nabla^2 + m_\sigma^2\right)\sigma = -g_\sigma\rho_S - g_2\sigma^2 - g_3\sigma^3$$

$$\left(-\nabla^2 + m_\omega^2\right)\omega = g_\omega\rho_V - c_3\omega^3$$

$$\left(-\nabla^2 + m_\rho^2\right)\rho = g_\rho\rho_3$$

$$-\nabla^2 A = e\rho_C$$

MDC-CDFT (β_{20}, β_{22}, β_{30}, β_{32}, β_{40}, …)

- Axially deformed harmonic oscillator (ADHO) basis

Ring_Gambhir_Lalazissis1997_CPC105-77

$$\left[-\frac{\hbar^2}{2M}\nabla^2 + V_B(z,\rho)\right]\Phi_\alpha(\boldsymbol{r}\sigma) = E_\alpha \Phi_\alpha(\boldsymbol{r}\sigma)$$

$$V_B(z,\rho) = \frac{1}{2}M(\omega_\rho^2\rho^2 + \omega_z^2 z^2)$$

$$\Phi_\alpha(\boldsymbol{r}\sigma) = C_\alpha \phi_{n_z}(z) R_{n_\rho}^{m_l}(\rho)\frac{1}{\sqrt{2\pi}} e^{i m_l \varphi}\chi_{s_z}(\sigma)$$

- Fourier expansion for densities & potentials

$$f(\rho,\varphi,z) = f_0(\rho,z)\frac{1}{\sqrt{2\pi}} + \sum_{n=1}^{\infty} f_n(\rho,z)\frac{1}{\sqrt{\pi}}\cos(2n\varphi)$$

$$f = V \text{ or } \rho$$

- A modified linear constraint method

$$E' = E_{\text{RMF}} + \sum_{\lambda\mu}\frac{1}{2}C_{\lambda\mu}Q_{\lambda\mu}$$

$$C_{\lambda\mu}^{(n+1)} = C_{\lambda\mu}^{(n)} + k_{\lambda\mu}\left(\beta_{\lambda\mu}^{(n)} - \beta_{\lambda\mu}\right)$$

Lu_Zhao_Zhao_SGZ 2014_PRC89-014323

MDC-CDFT (β_{20}, β_{22}, β_{30}, β_{32}, β_{40}, …)

ph channel	Non-linear	Density-dependent
Meson exchange	NL3, NL3*, PK1, …	DD-ME1, DD-ME2, …
Point Coupling	PC-F1, PC-PK1, …	DD-PC1, …

MDC-RMF

MDC-RHB

pp channel	BCS	Bogoliubov
Constant gap	√	
Constant strength	√	
Delta force	√	√
Separable force	√	√

Lu_Zhao_SGZ 2011_PRC84-014328

Lu_Zhao_SGZ 2012_PRC85-011301R

Zhao_Lu_Zhao_SGZ 2012_PRC86-057304

Lu_Zhao_Zhao_SGZ 2014_PRC89-014323

Numerical checks

- $(\beta_2, \beta_3, \ldots)$

  Geng_Meng_Toki2007_ChinPhysLett24-1865

- $(\beta_2, \gamma, \ldots)$

  Meng_Peng_Zhang_SGZ2006_PRC73-037303

- $(\beta_2, \ldots)$

  Ring_Gambhir_Lalazissis1997_CPC105-77

Lu_Zhao_SGZ 2011_PRC84-014328

Lu_Zhao_SGZ 2012_PRC85-011301R

Zhao_Lu_Zhao_SGZ 2012_PRC86-057304

Lu_Zhao_Zhao_SGZ 2014_PRC89-014323

Numerical checks

- $(\beta_2, \beta_3, \ldots)$

  Geng_Meng_Toki2007_ChinPhysLett24-1865

- $(\beta_2, \gamma, \ldots)$

  Meng_Peng_Zhang_SGZ2006_PRC73-

- $(\beta_2, \ldots)$

  Ring_Gambhir_Lalazissis1997_CPC105

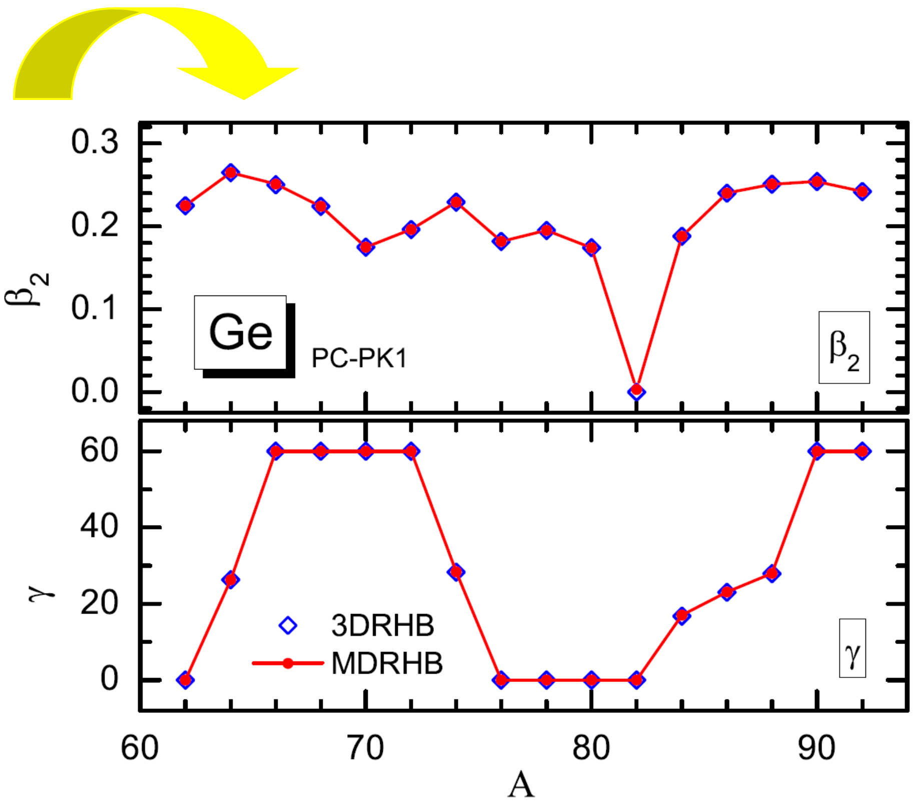

Lu_Zhao_SGZ 2011_PRC84-014328

Lu_Zhao_SGZ 2012_PRC85-011301R

Zhao_Lu_Zhao_SGZ 2012_PRC86-057304

Lu_Zhao_Zhao_SGZ 2014_PRC89-014323

Numerical checks

- $(\beta_2, \beta_3, \ldots)$

  Geng_Meng_Toki2007_ChinPhysLett24-186

- $(\beta_2, \gamma, \ldots)$

  Meng_Peng_Zhang_SGZ2006_PRC73-0373

- $(\beta_2, \ldots)$

  Ring_Gambhir_Lalazissis1997_CPC105-77

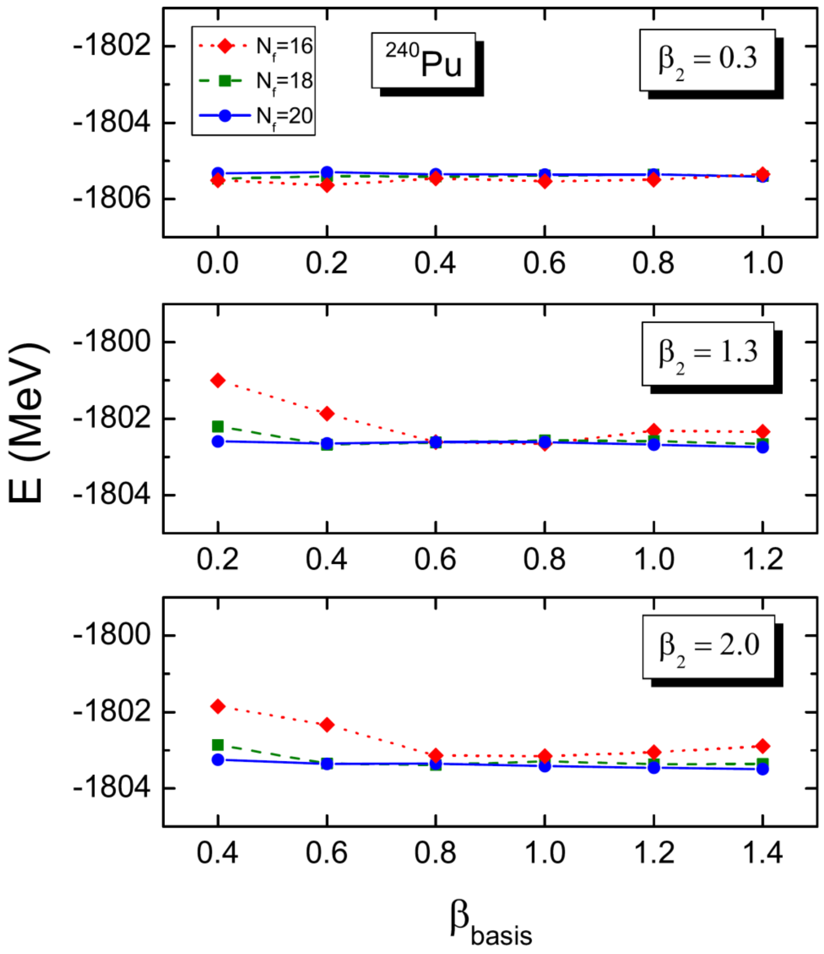

Larger basis size in the elongated direction

Warda_Egido_Robledo_Pomorski 2002_PRC66-014310

Lu_Zhao_SGZ 2011_PRC84-014328

Lu_Zhao_SGZ 2012_PRC85-011301R

Zhao_Lu_Zhao_SGZ 2012_PRC86-057304

Lu_Zhao_Zhao_SGZ 2014_PRC89-014323

Numerical checks

- (β_2, β_3, ...)

  Geng_Meng_Toki2007_ChinPhysLett24-18(

- (β_2, γ, ...)

  Meng_Peng_Zhang_SGZ2006_PRC73-0373

- (β_2, ...)

  Ring_Gambhir_Lalazissis1997_CPC105-77

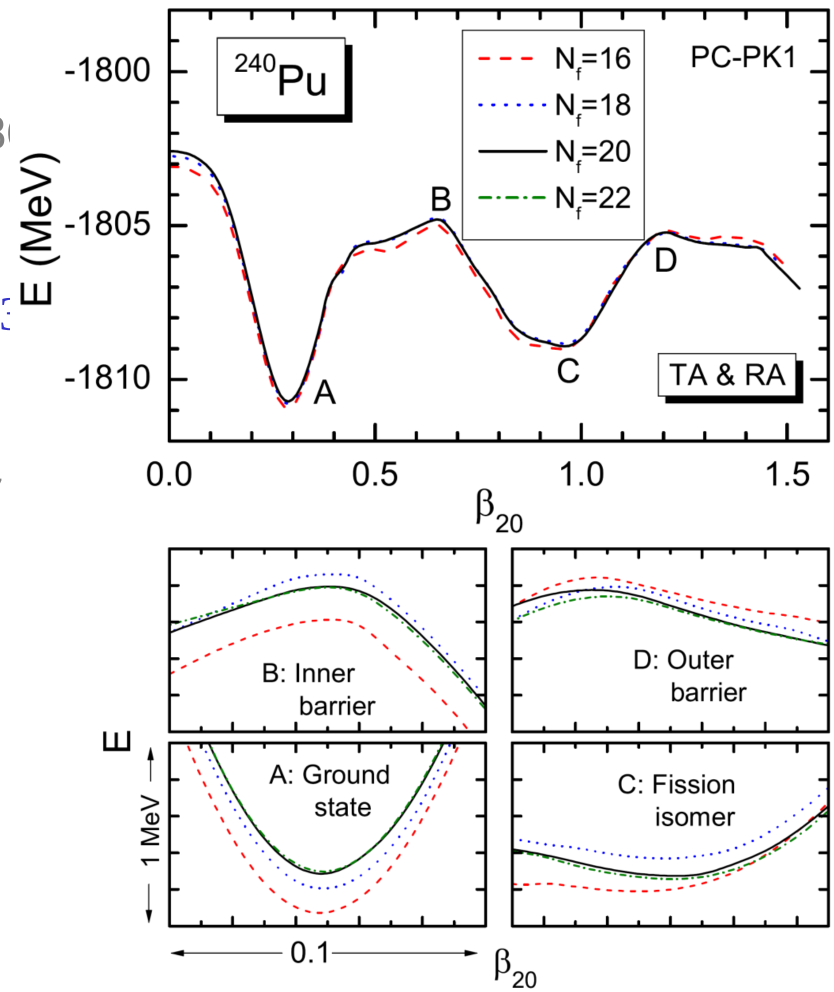

Convergence of the binding energy w.r.t. the size of the ADHO basis

Lu_Zhao_SGZ 2011_PRC84-014328

Lu_Zhao_SGZ 2012_PRC85-011301R

Zhao_Lu_Zhao_SGZ 2012_PRC86-057304

Lu_Zhao_Zhao_SGZ 2014_PRC89-014323

Numerical checks

- $(\beta_2, \beta_3, \ldots)$

  Geng_Meng_Toki2007_ChinPhysLett24-1865

- $(\beta_2, \gamma, \ldots)$

  Meng_Peng_Zhang_SGZ2006_PRC73-

- $(\beta_2, \ldots)$

  Ring_Gambhir_Lalazissis1997_CPC10

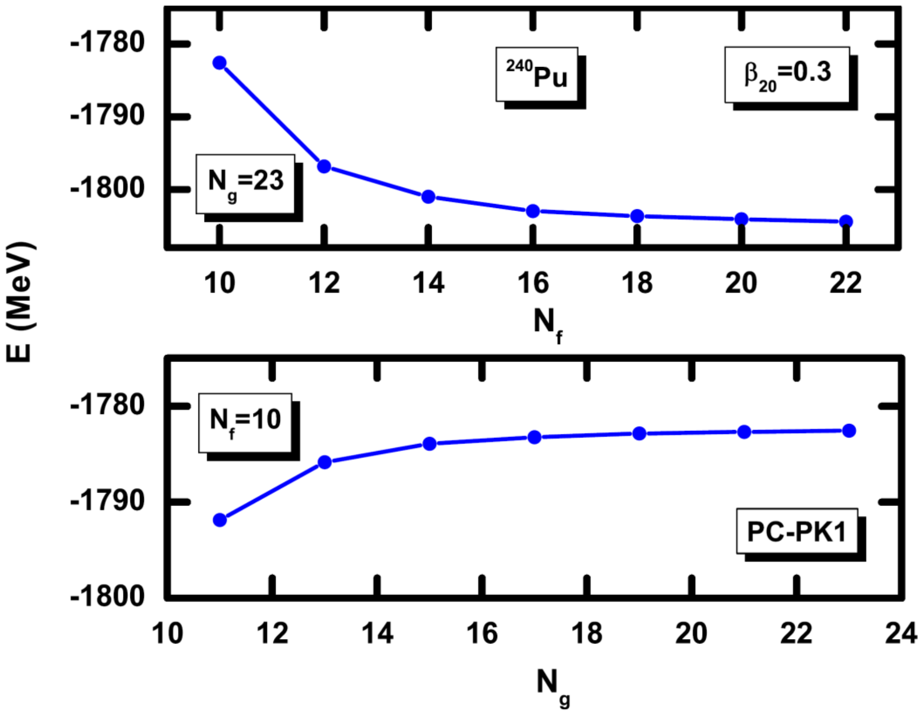

The “variational collapse” problem

Kutzelnigg1984_IJQuanChem25-107

Lu_Zhao_SGZ 2011_PRC84-014328

Lu_Zhao_SGZ 2012_PRC85-011301R

Zhao_Lu_Zhao_SGZ 2012_PRC86-057304

Lu_Zhao_Zhao_SGZ 2014_PRC89-014323

Potential energy surface: an example

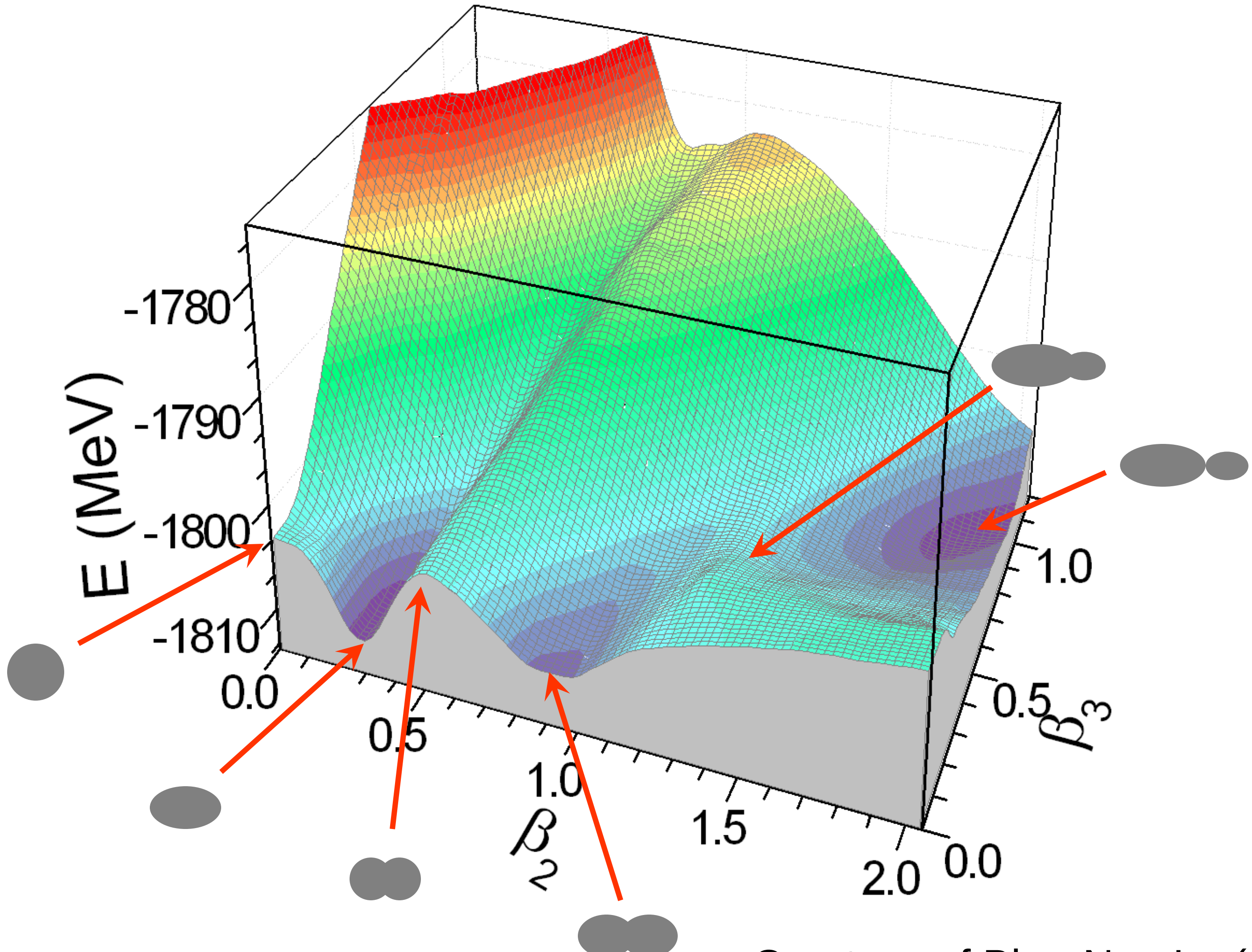

Courtesy of Bing-Nan Lu (吕炳楠)

Potential energy surface: an example

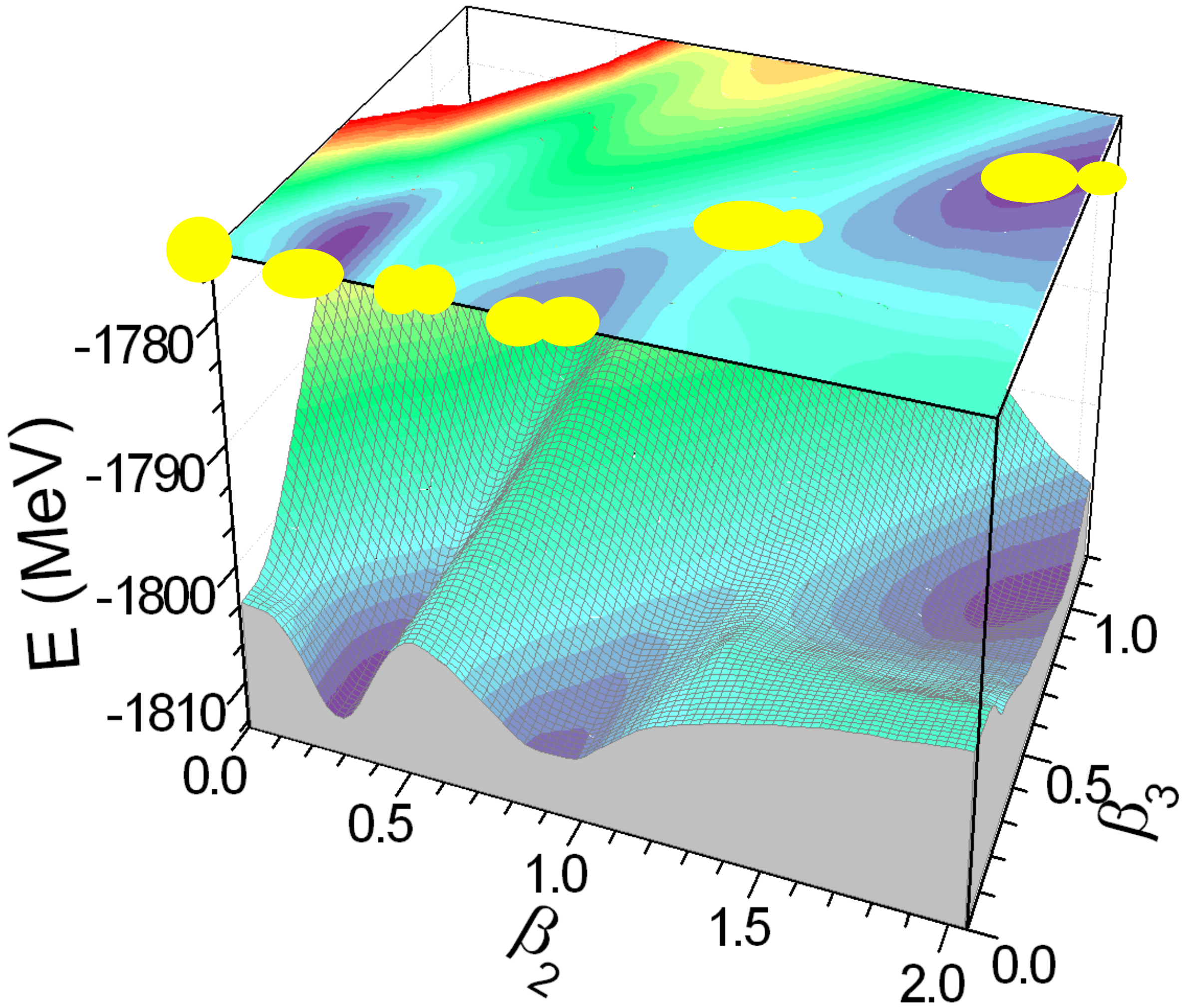

Courtesy of Bing-Nan Lu (吕炳楠)

^{240}Pu: 1-dim. potential energy curve (β_{20})

- Triaxiality lowers inner barrier height by more than 2 MeV
- Octupole deformation lowers outer barrier dramatically
- Triaxiality lowers outer barrier height by about 1 MeV

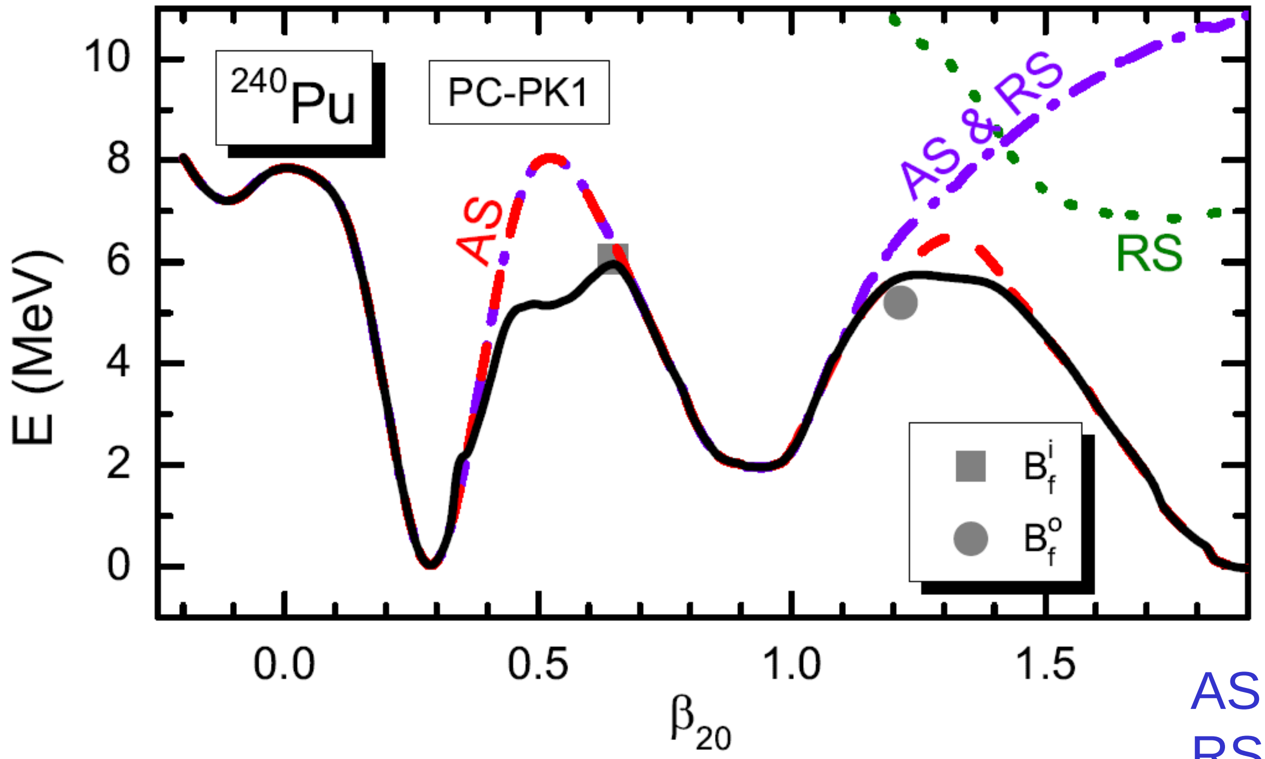

AS: Axially Sym.
RS: Reflection Sym.

Lu_Zhao_SGZ 2012_PRC85-011301R

^{240}Pu: 2-dim. PES (β_{20}, β_{30})

Without triaxility

With triaxility

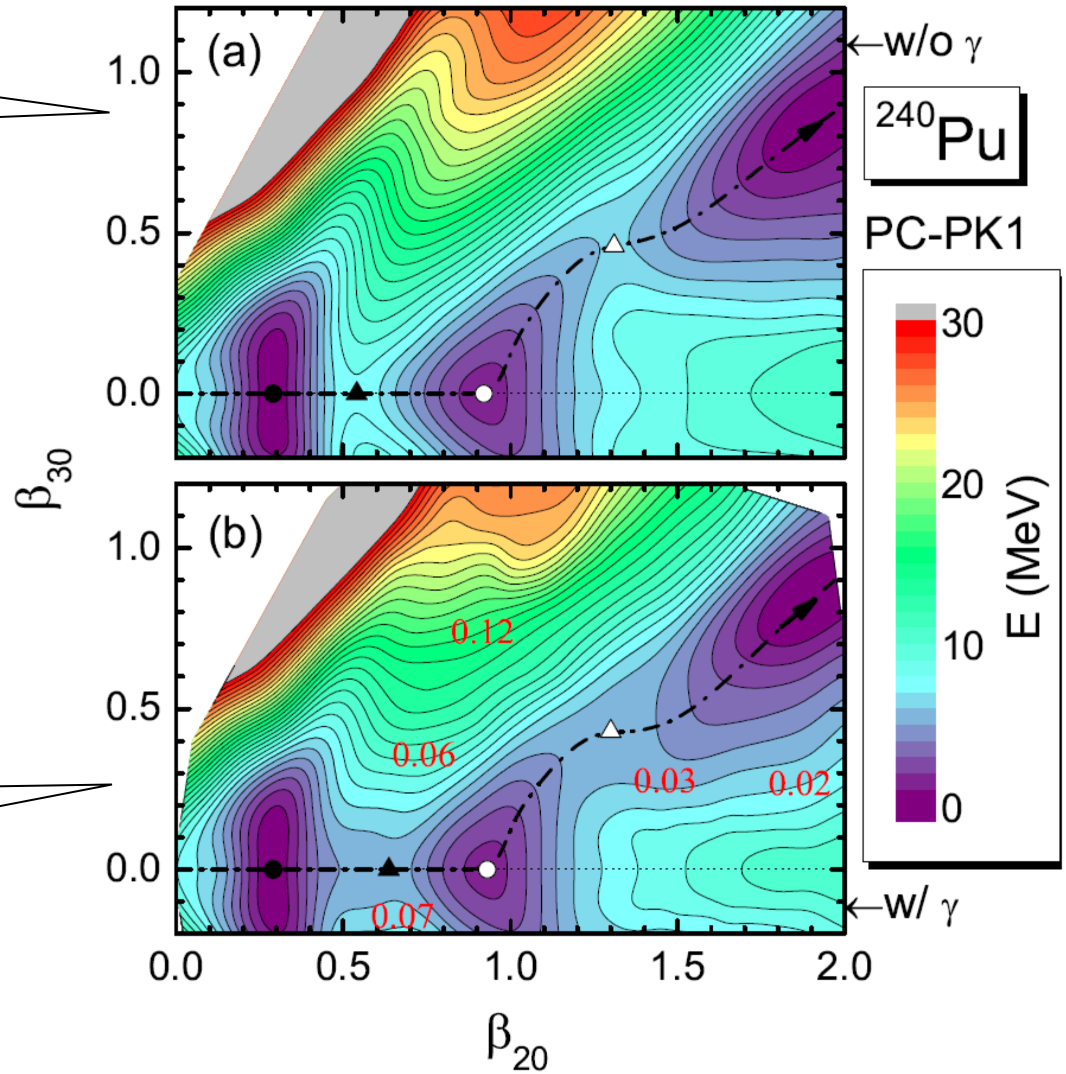

Lu_Zhao_SGZ 2012_PRC85-011301R

^{240}Pu: 3-dim. PES (β_{20}, β_{22}, β_{30})

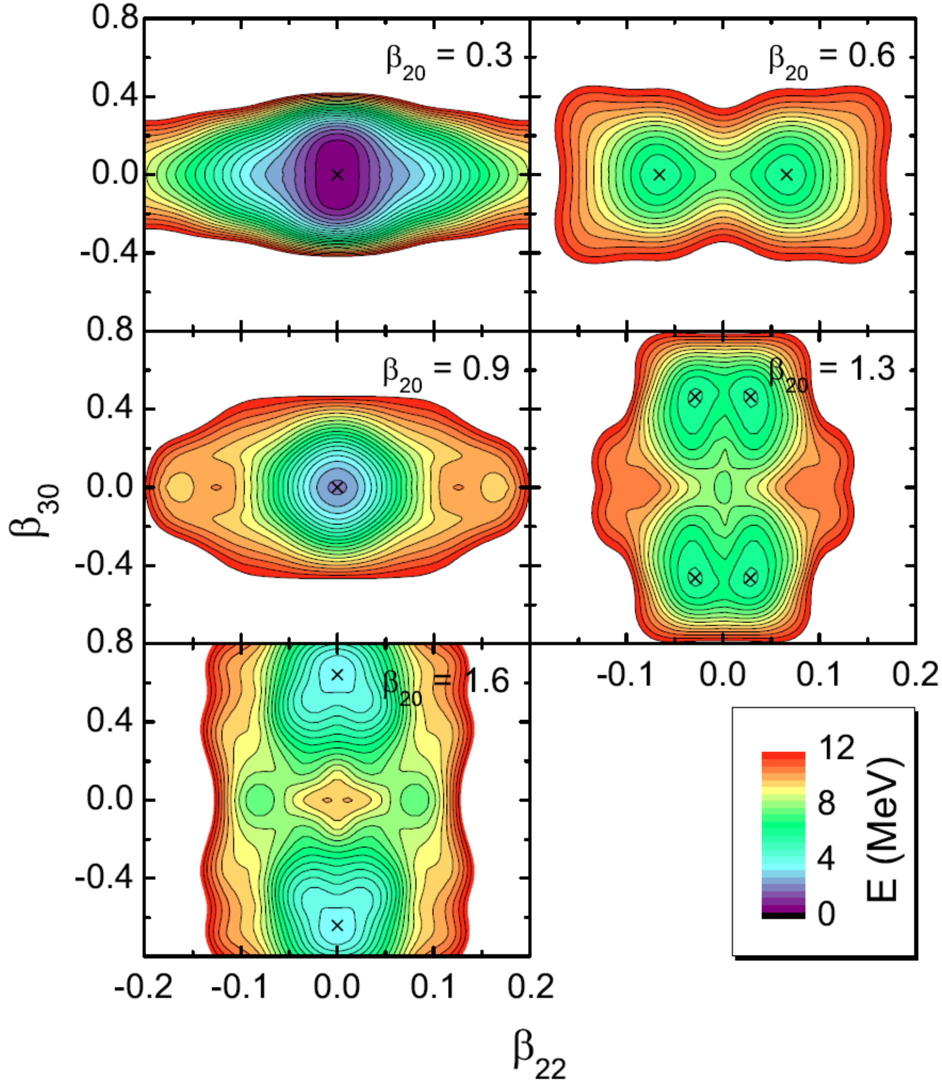

- AS & RS for g.s. & isomer, the latter is stiffer
- Triaxial & octupole shape around the outer barrier
- Triaxial deformation crucial around barriers

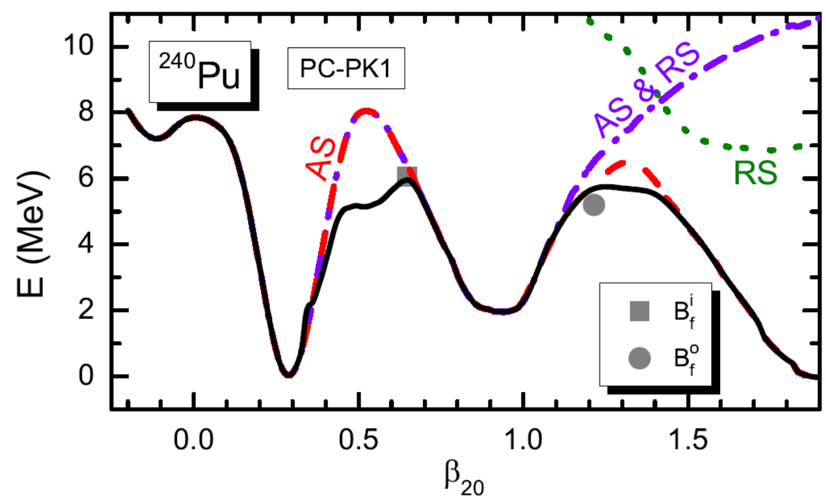

Lu_Zhao_SGZ 2012_PRC85-011301R

B_f of actinide nuclei

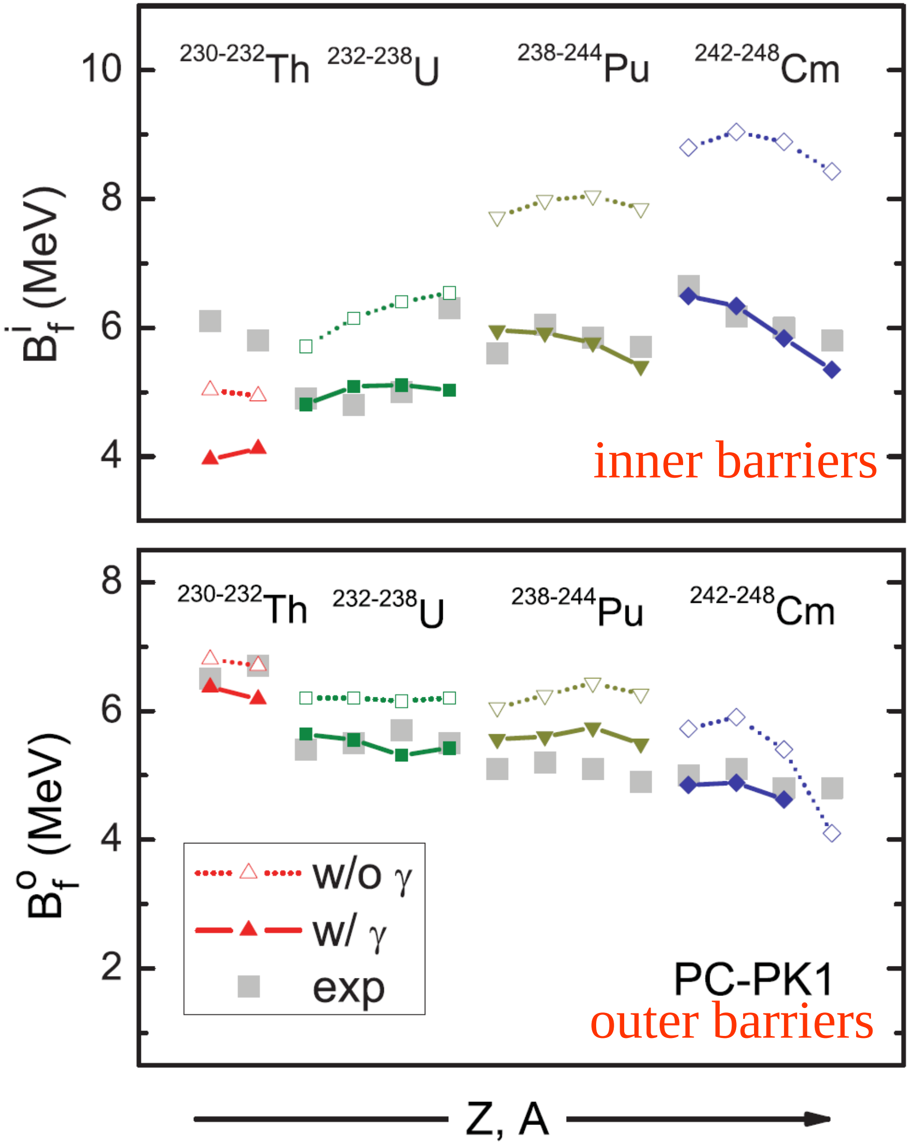

- Influence of triaxiality
  - Inner fission barriers lowered by 1~2 MeV
  - Outer fission barriers lowered by 0.5~1 MeV
- Problems
  - $^{230-232}$Th: out barriers primary
  - ^{238}U: ?
  - ^{248}Cm: two fission paths

Empirical values: RIPL-3 (NDS2010)

Lu_Zhao_SGZ 2012_PRC85-011301R

Non-axial octupole shape in *N* = 150 isotones

Skalski1991_PRC43-140
Hamamoto_Mottelson_Xie_Zhang1991_ZPD21-163
Li_Dudek1994_PRC49-1250R
Takami_Yabana_Matsuo1998_PLB431-242
…

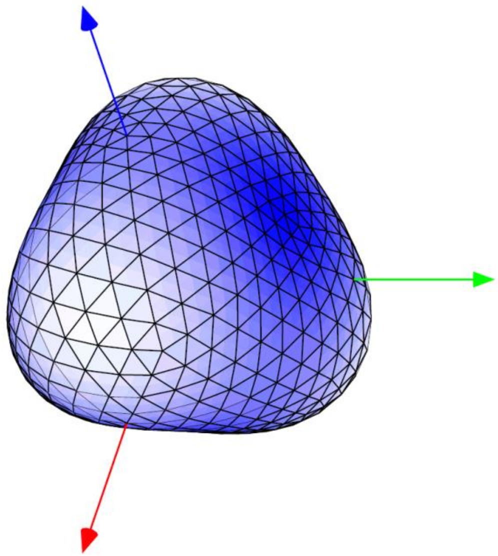

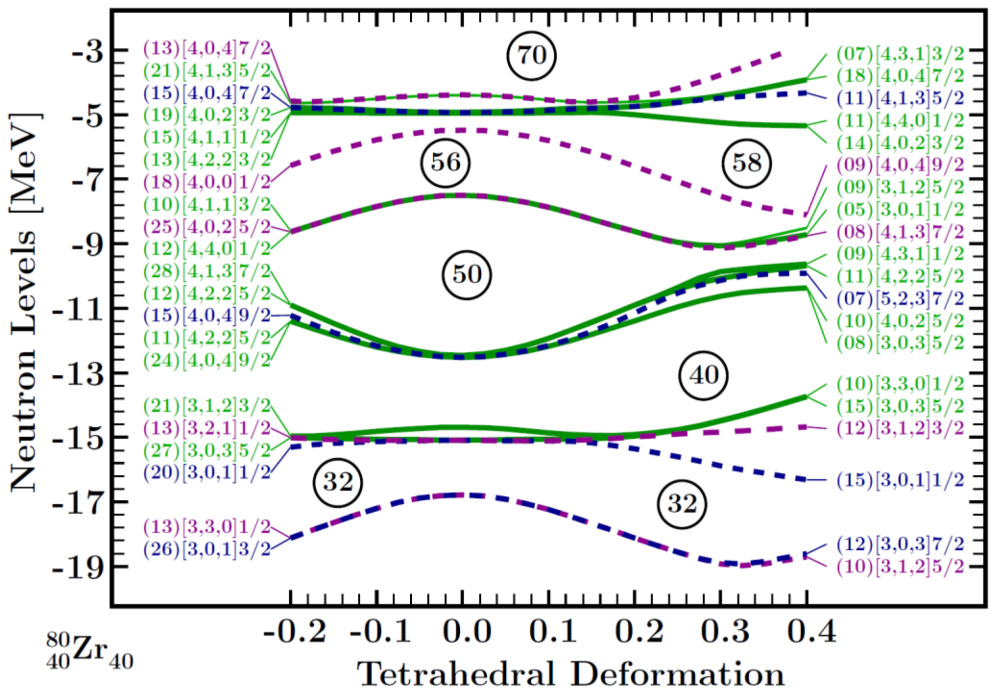

Dudek_Gozdz_Mazur_Molique_Rybak_Fornal
2010_JPG37-064032

Non-axial octupole shape in $N = 150$ isotones

PHYSICAL REVIEW C **77**, 061305(R) (2008)

Nonaxial-octupole effect in superheavy nuclei

Y.-S. Chen,[1] Yang Sun,[2,3] and Zao-Chun Gao[1,4]

[1]*China Institute of Atomic Energy, P. O. Box 275(18), Beijing 102413, People's Republic of China*
[2]*Department of Physics, Shanghai Jiao Tong University, Shanghai 200240, People's Republic of China*
[3]*Joint Institute for Nuclear Astrophysics, University of Notre Dame, Notre Dame, Indiana 46556, USA*
[4]*Department of Physics, Central Michigan University, Mount Pleasant, Michigan 48859, USA*

(Received 26 March 2008; published 26 June 2008)

The triaxial-octupole Y_{32} correlation in atomic nuclei has long been expected to exist but experimental evidence has not been clear. We find, in order to explain the very low-lying 2^- bands in the transfermium mass region, that this exotic effect may manifest itself in superheavy elements. Favorable conditions for producing triaxial-octupole correlations are shown to be present in the deformed single-particle spectrum, which is further supported by quantitative Reflection Asymmetric Shell Model calculations. It is predicted that the strong nonaxial-octupole effect may persist up to the element 108. Our result thus represents the first concrete example of spontaneous breaking of both axial and reflection symmetries in the heaviest nuclear systems.

Non-axial octupole shape in *N* = 150 isotones

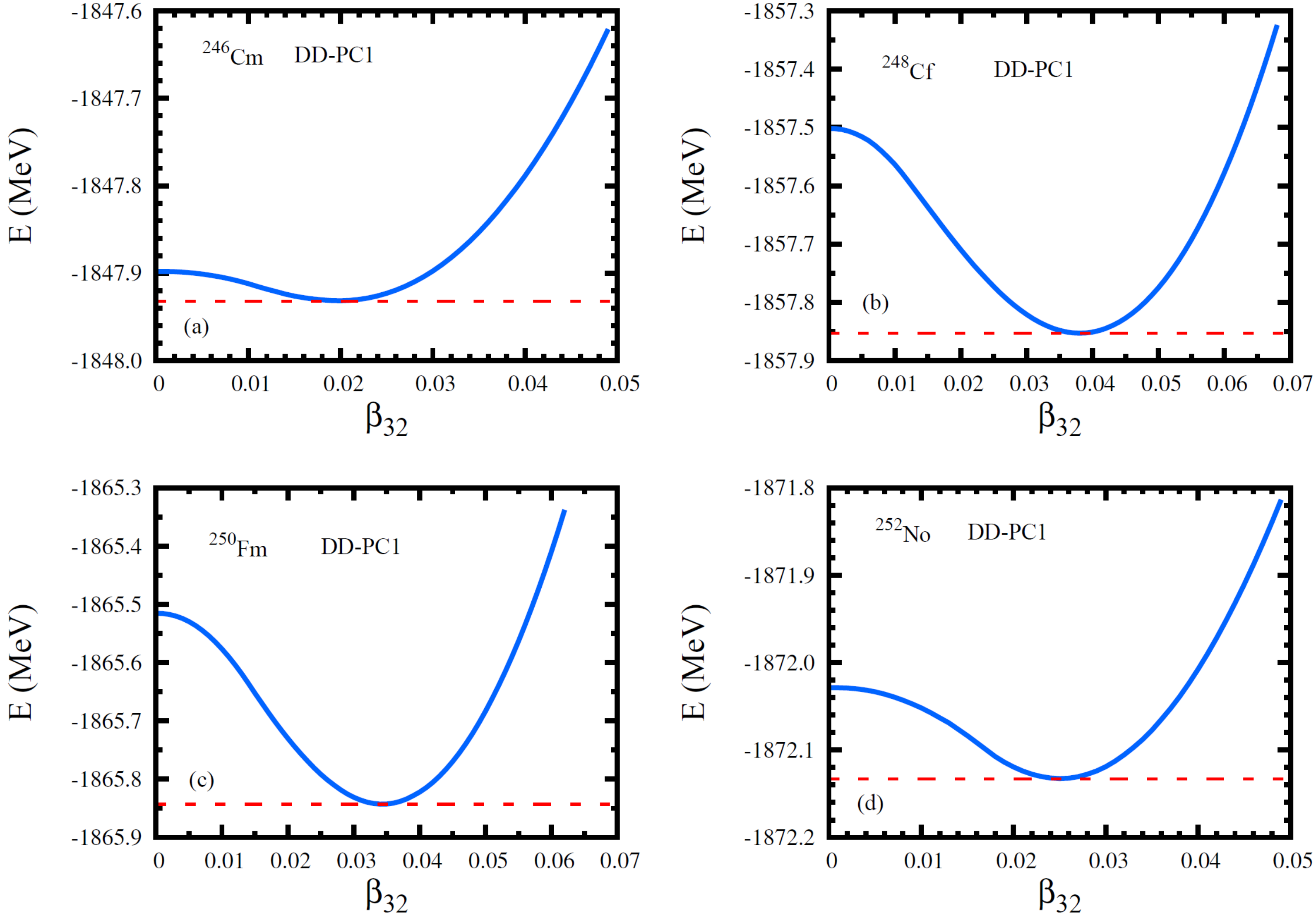

Zhao_Lu_Zhao_SGZ2012 PRC86-057304

Non-axial octupole shape in *N* = 150 isotones

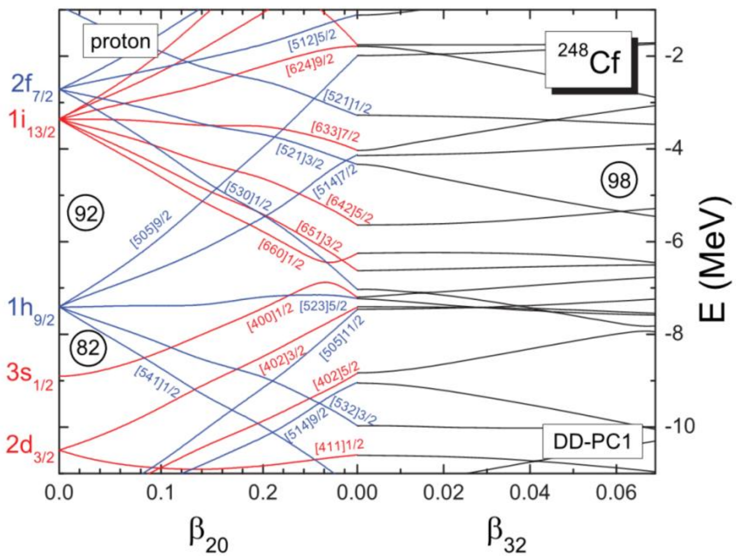

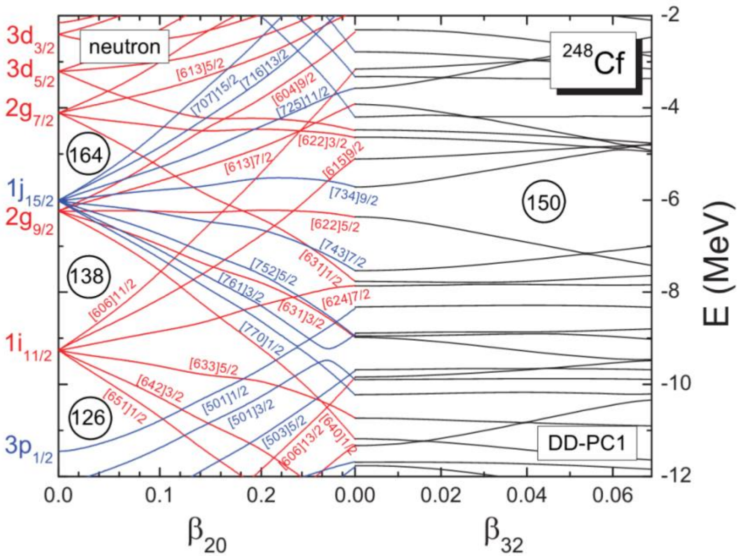

- Y_{32} correlations from near degeneracy of pair of orbitals with $\Delta l = \Delta j = 3$ & $\Delta K = 2$

- For ^{248}Cf
  - ➢ $\pi 7/2[633]$ ($1i_{13/2}$) & $\pi 3/2[521]$ ($2f_{7/2}$)
  - ➢ $\nu 9/2[734]$ ($1j_{15/2}$) & $\nu 5/2[622]$ ($2g_{9/2}$)

Zhao_Lu_Zhao_SGZ2012 PRC86-057304

Hyperdeformed shapes in actinides

Moller1972_NPA192-529

…

Blons_Mazur_Paya1975_PRL35-1749

…

Cwiok_Nazarewicz_Saladin_Plociennik_Johnson1994_PLB322-304

…

Csige et al. 2013_PRC87-044321

…

Kowal_Skalski2012_PRC85-061302R

Jochimowicz_Kowal_Skalski2013_PRC87-044308

Ichikawa_Moller_Sierk2013_PRC87-054326

McDonnell_Nazarewicz_Sheikh2013_PRC87-054327

…

Hyperdeformed shapes in actinides

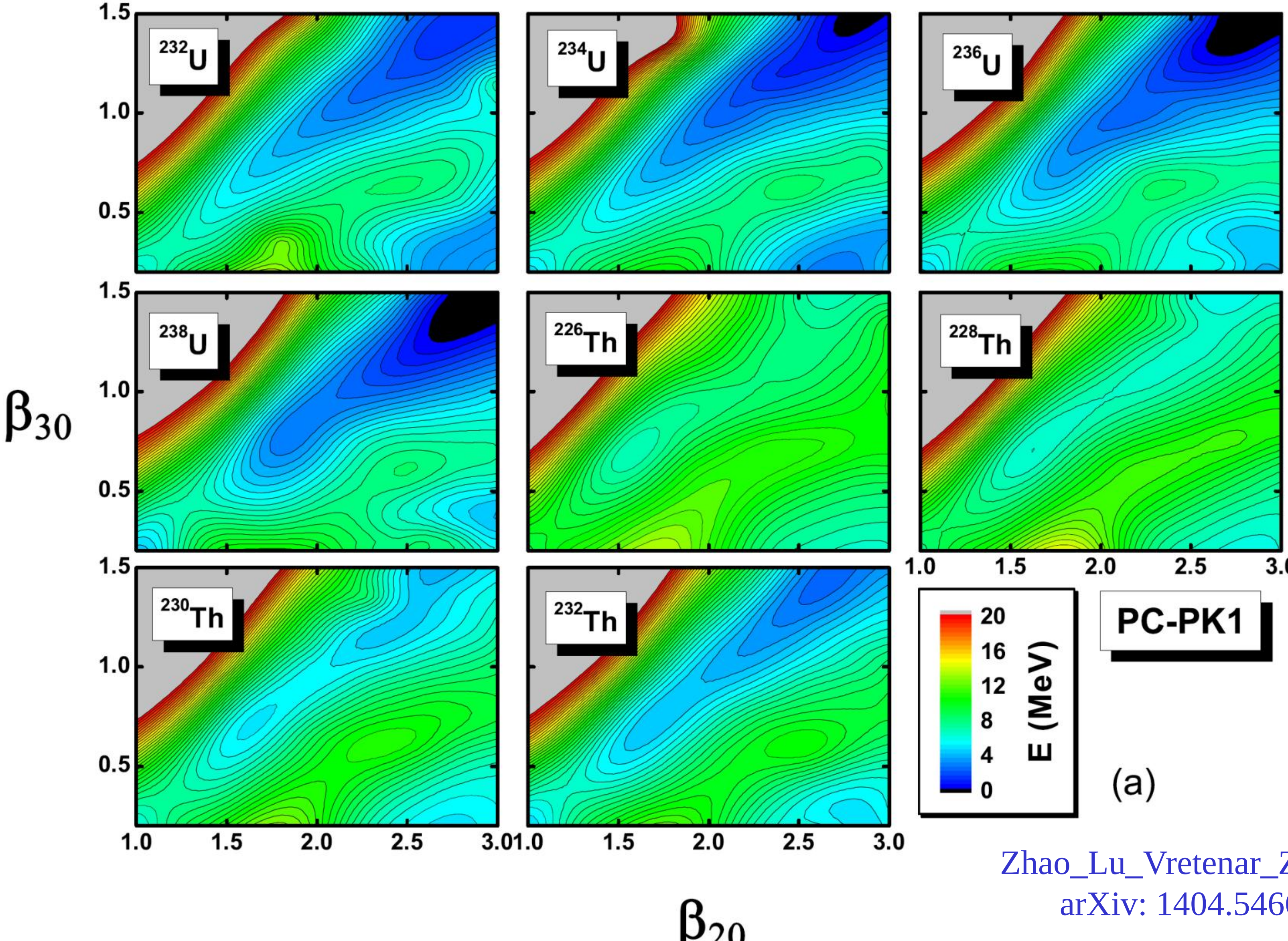

Zhao_Lu_Vretenar_Zhao_SGZ
arXiv: 1404.5466 [nucl-th]

Hyperdeformed shapes in actinides

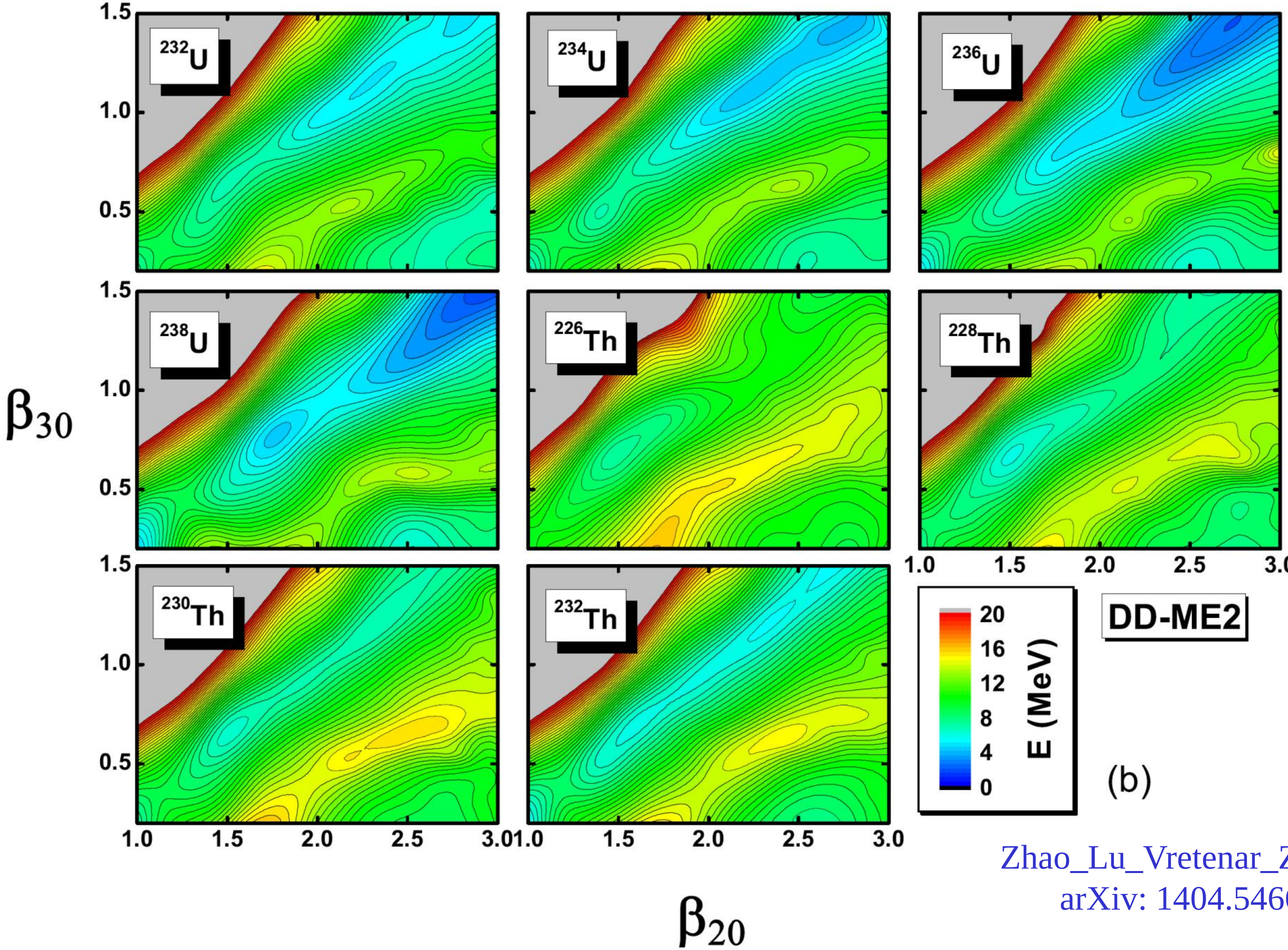

Zhao_Lu_Vretenar_Zhao_SGZ
arXiv: 1404.5466 [nucl-th]

Hyperdeformed shapes in actinides

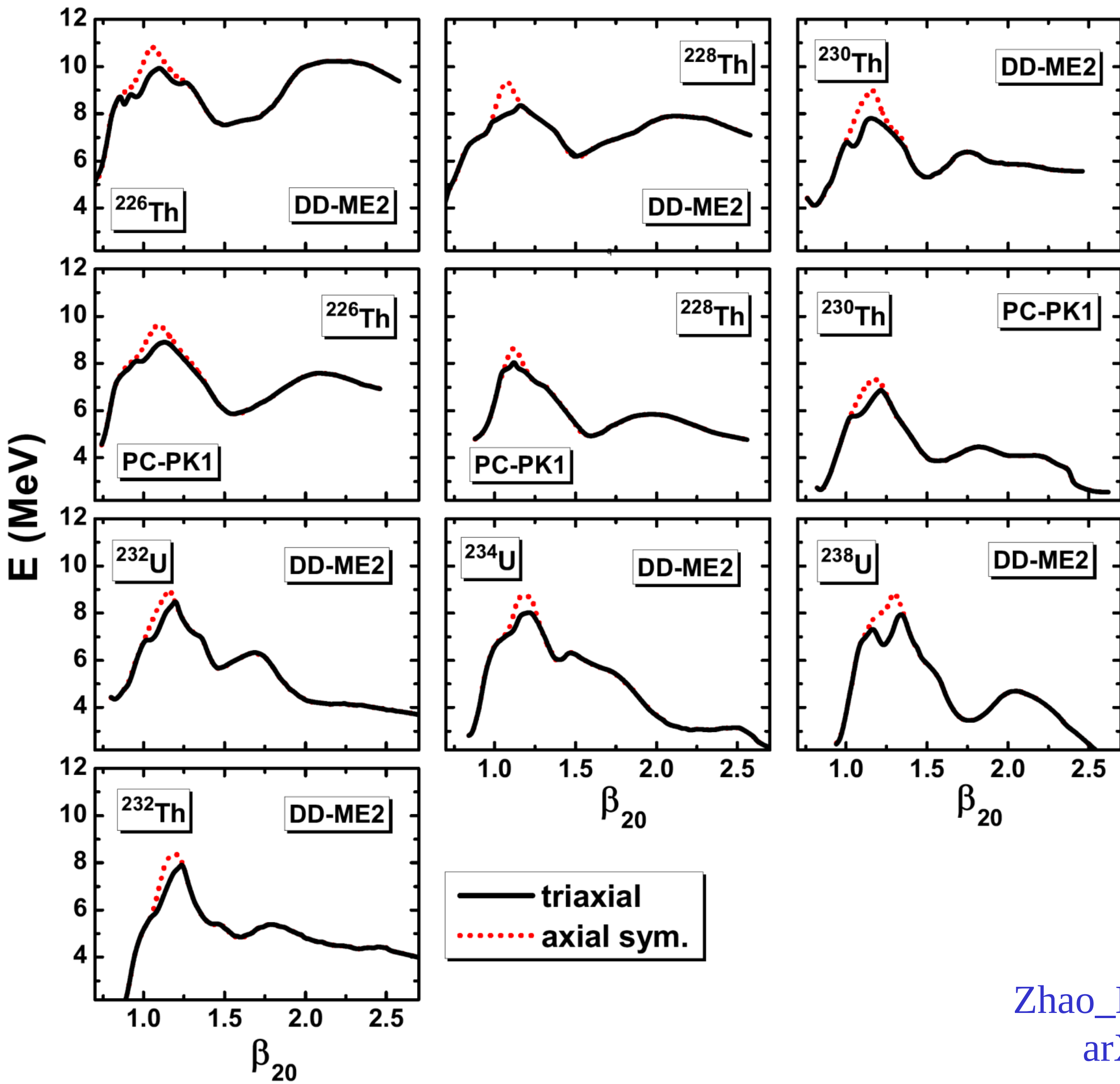

Zhao_Lu_Vretenar_Zhao_SGZ
arXiv: 1404.5466 [nucl-th]

Shapes of Λ hypernuclei w/ MF models

- Non-relativistic mean field study of hypernuclei
  - An axially deformed Skyrme Hartree-Fock (SHF) model
  - Similar shapes of core nuclei & the corresponding hypernuclei

Zhou_Schulze_Sagawa_Wu_Zhao2007_PRC76-034312

- However, a RMF study reveals
  - In most cases the results are similar to the SHF calculations
  - Several exceptions, e.g., ${}^{13}_{\Lambda}C$ & ${}^{29}_{\Lambda}Si$ whose shapes change dramatically compared to their corresponding core nuclei

Win_Hagino2008_PRC78-054311

- Different polarization effect of Λ in SHF & RMF

Schulze_Win_Hagino_Sagawa2010_PTP123-569

Triaxiality in hypernuclei w/ RMF model

	Skyrme HF	RMF
Spherical	Yes	Yes
Axially deformed	Yes	Yes
Triaxially deformed	Yes	???

Triaxially defromed RMF: With an additional Λ, no significant shape change occurs except that the PES becomes softer in the γ direction

Win_Hagino_Koike2011_PRC83-014301

What RMF models predict for trixiality in hypernuclei?

RMF model for Λ hypernuclei

- The Lagrangian density: $\mathcal{L} = \mathcal{L}_0 + \mathcal{L}_\Lambda$

$$\mathcal{L}_\Lambda = \bar{\psi}_\Lambda \left(i\gamma^\mu \partial_\mu - m_\Lambda - g_{\sigma\Lambda}\sigma - g_{\omega\Lambda}\gamma^\mu \omega_\mu \right) \psi_\Lambda + \frac{f_{\omega\Lambda\Lambda}}{4m_\Lambda} \bar{\psi}_\Lambda \sigma^{\mu\nu} \Omega_{\mu\nu} \psi_\Lambda,$$

- The Dirac equation for Λ

$$\left[\vec{\alpha} \cdot \vec{p} + \beta \left(m_\Lambda + S_\Lambda \right) + V_\Lambda + T_\Lambda \right] \psi_{\Lambda i} = \epsilon_i \psi_{\Lambda i}$$

$$T_\Lambda = -\frac{f_{\omega\Lambda\Lambda}}{2m_\Lambda} \beta \left(\vec{\alpha} \cdot \vec{p} \right) \omega$$

- Effective interactions

Parameter	m_Λ	$g_{\sigma\Lambda}$	$g_{\omega\Lambda}$	$f_{\omega\Lambda\Lambda}$	N-N interaction
PK1-Y1	1115.6 MeV	$0.580 g_\sigma$	$0.620 g_\omega$	$-g_{\omega\Lambda}$	PK1
NLSH-A	1115.6 MeV	$0.621 g_\sigma$	$0.667 g_\omega$	$-g_{\omega\Lambda}$	NLSH

PK1-Y1: Song_Yao_Lü_Meng2010_IJMPE19-2538
Wang_Sang_Wang_Lü2014_Commu.Theor.Phys.60-479
NLSH-A: Win_Hagino2008_PRC78-054311

Carbon isotopes: w/ & w/o Λ

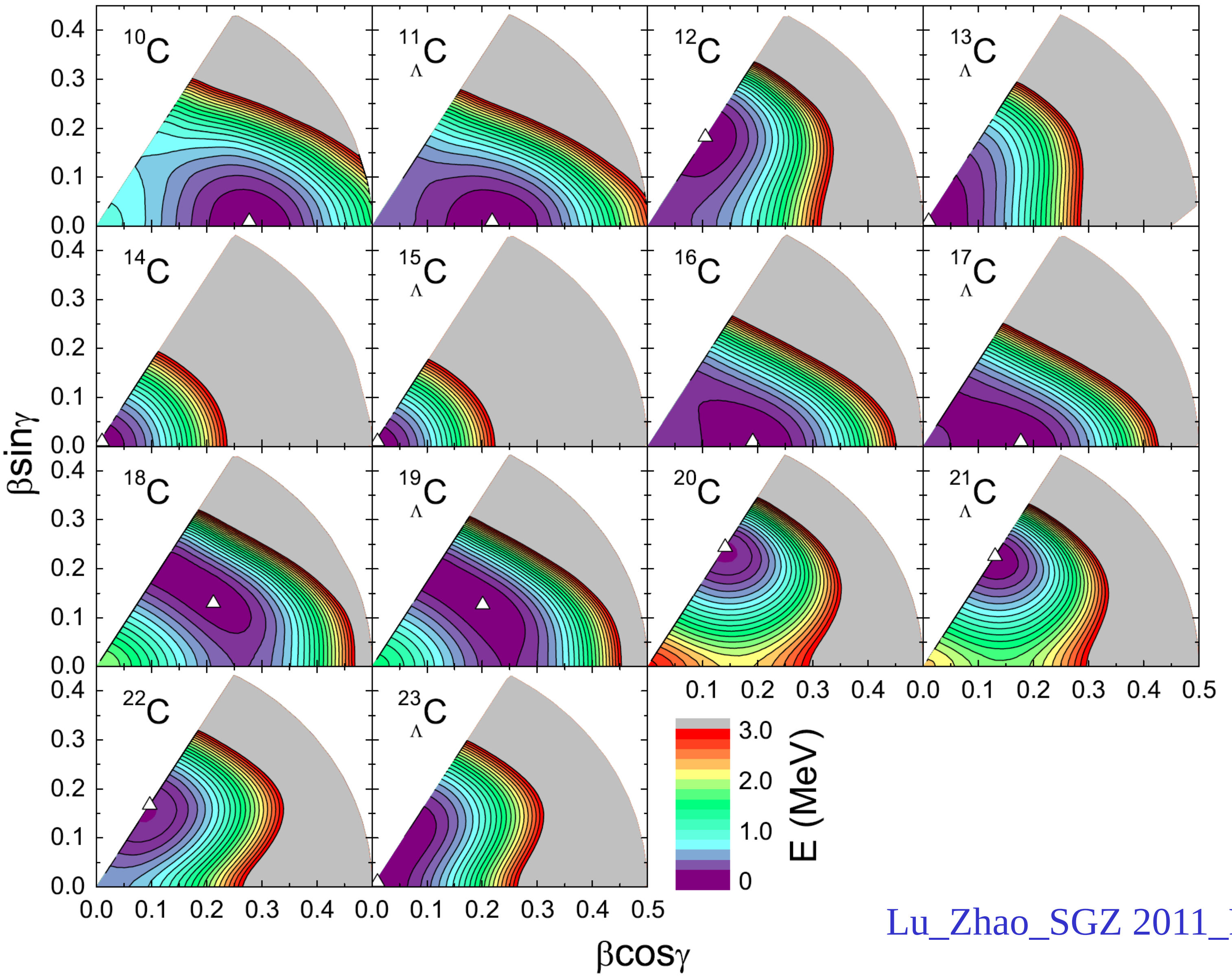

Lu_Zhao_SGZ 2011_PRC84-014328

Potential energy surfaces of ^{12}C & $^{13}_{\Lambda}C$

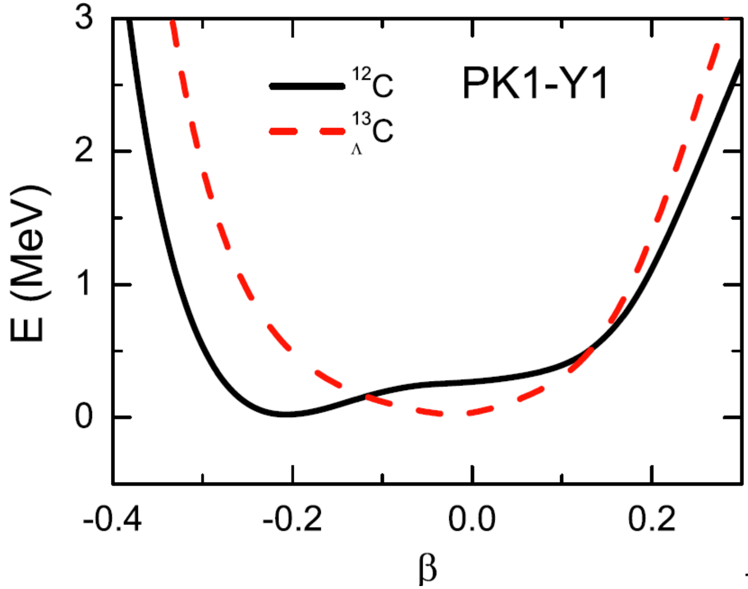

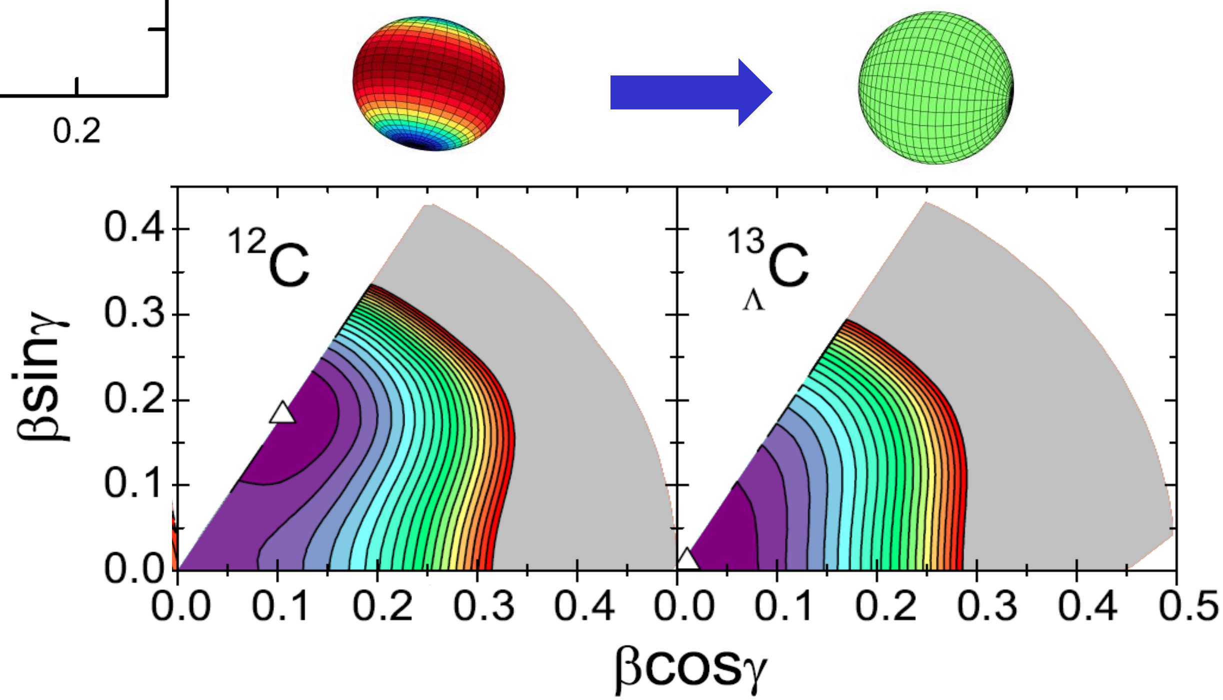

Lu_Zhao_SGZ 2011_PRC84-014328

Silicon isotopes: w/ & w/o Λ

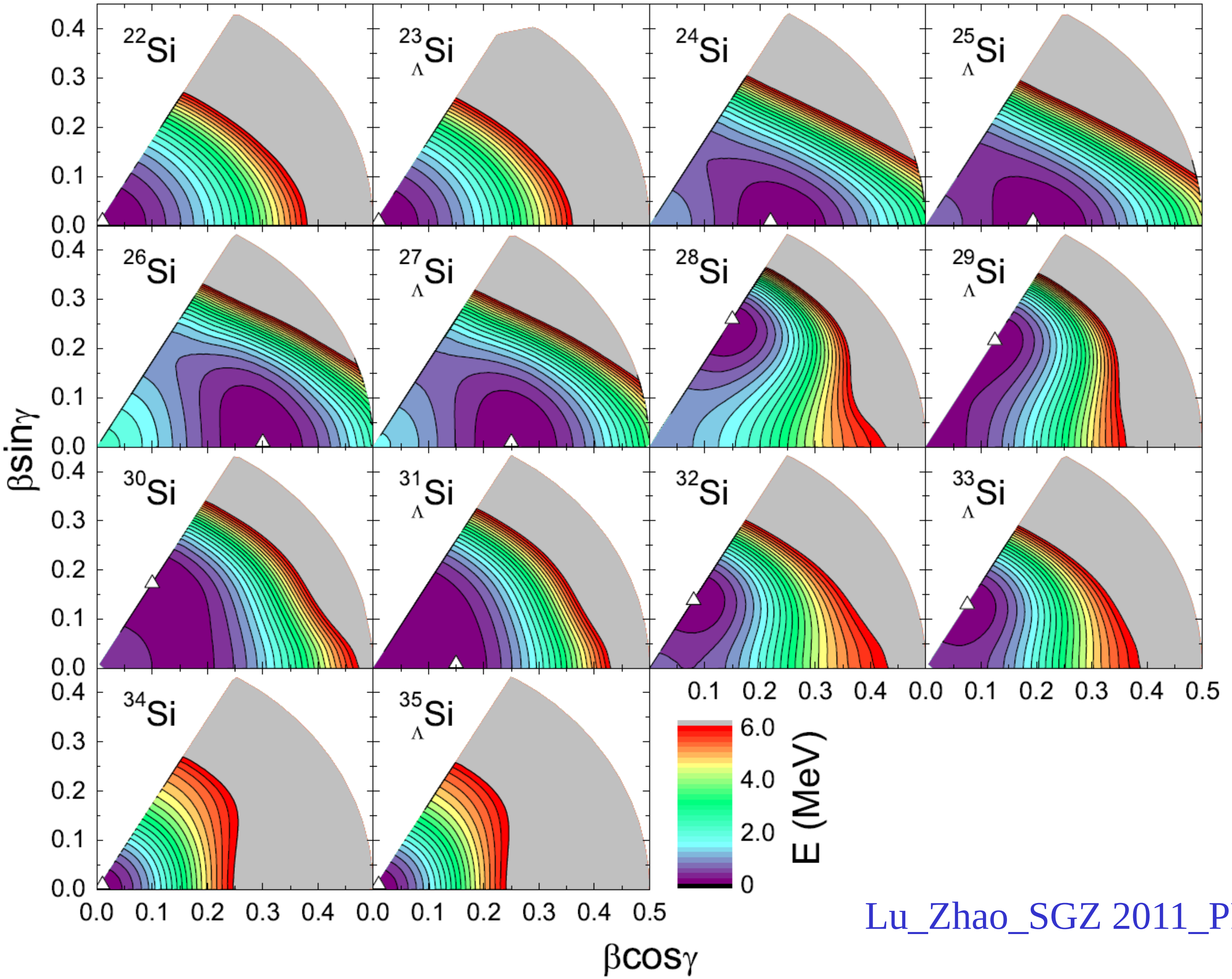

Lu_Zhao_SGZ 2011_PRC84-014328

Potential energy surfaces of ^{28}Si & $^{29}_{\Lambda}$Si

Model dependence
Parameter dependence

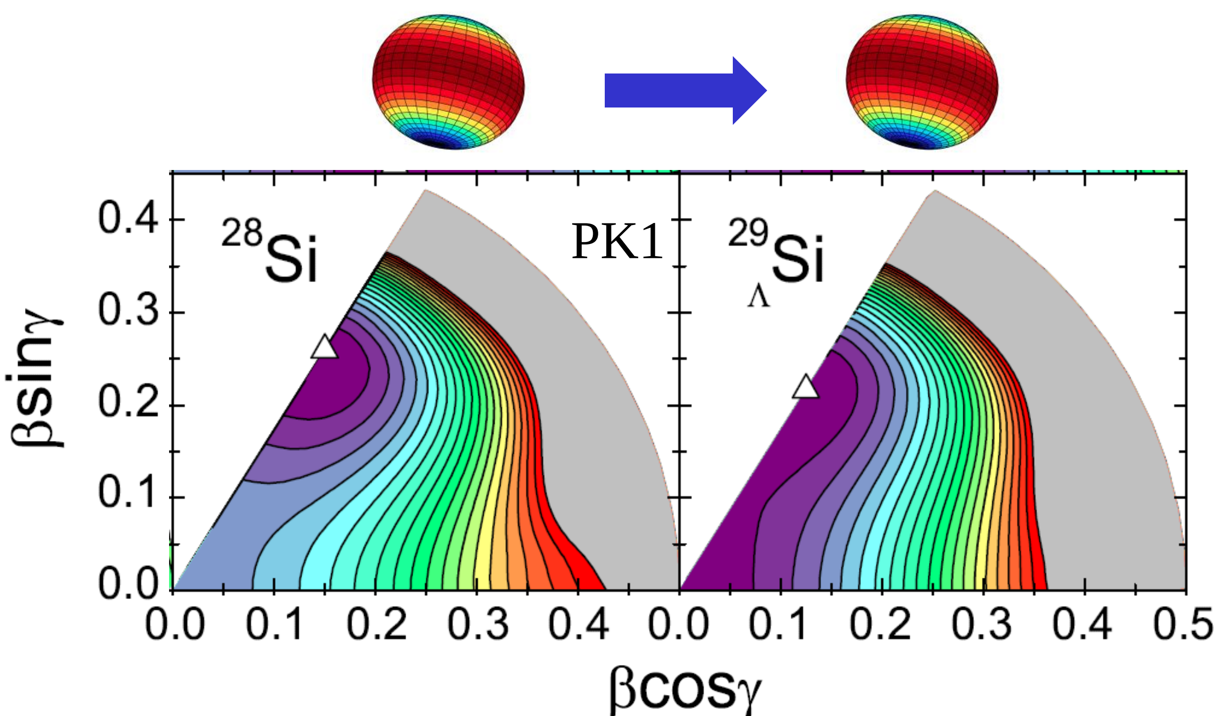

Lu_Zhao_SGZ 2011_PRC84-014328

Potential energy surfaces of ^{28}Si & $^{29}{}_{\Lambda}$Si

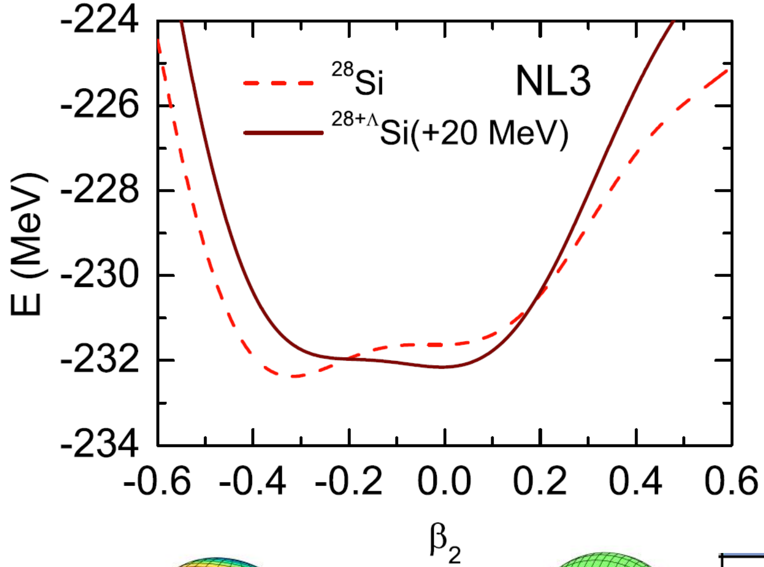

Model dependence

Parameter dependence

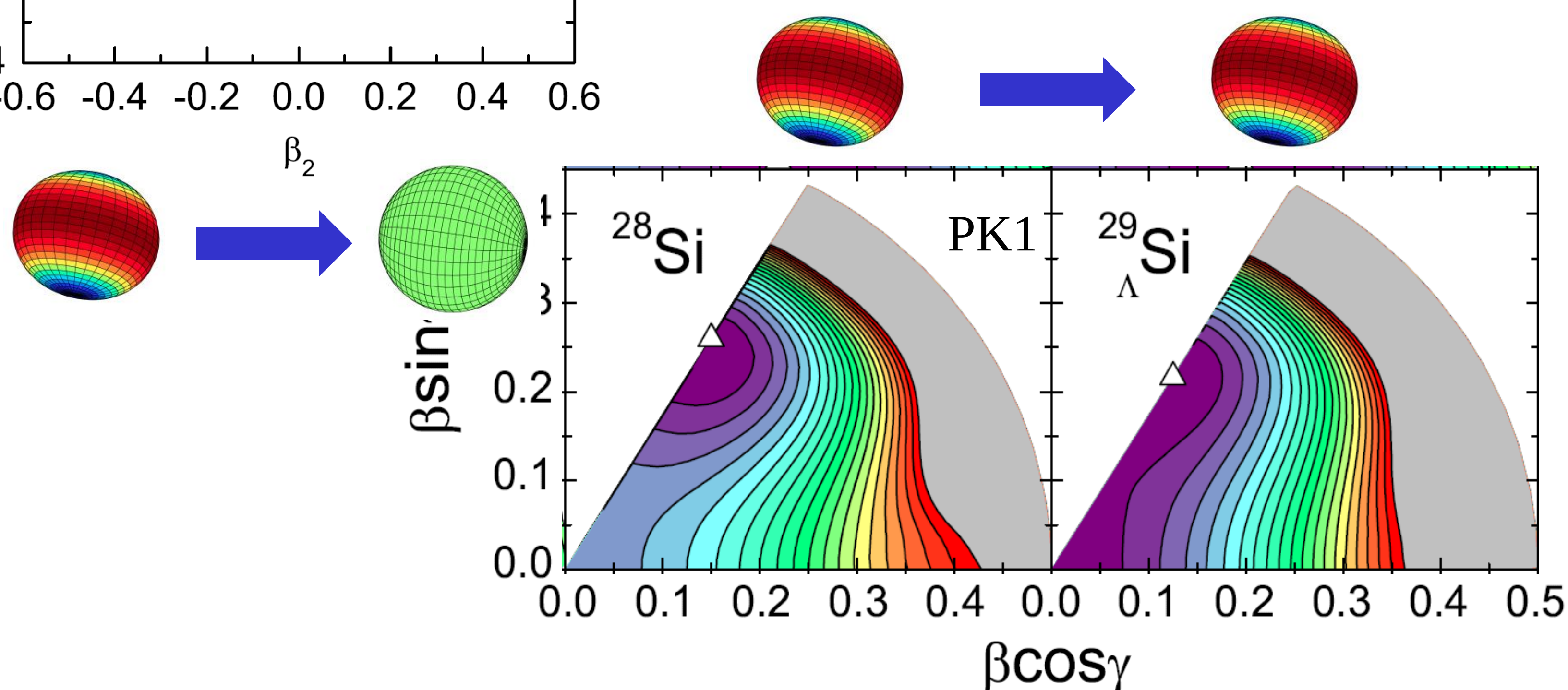

Lu_Zhao_SGZ 2011_PRC84-014328

Superdeformed hypernuclei

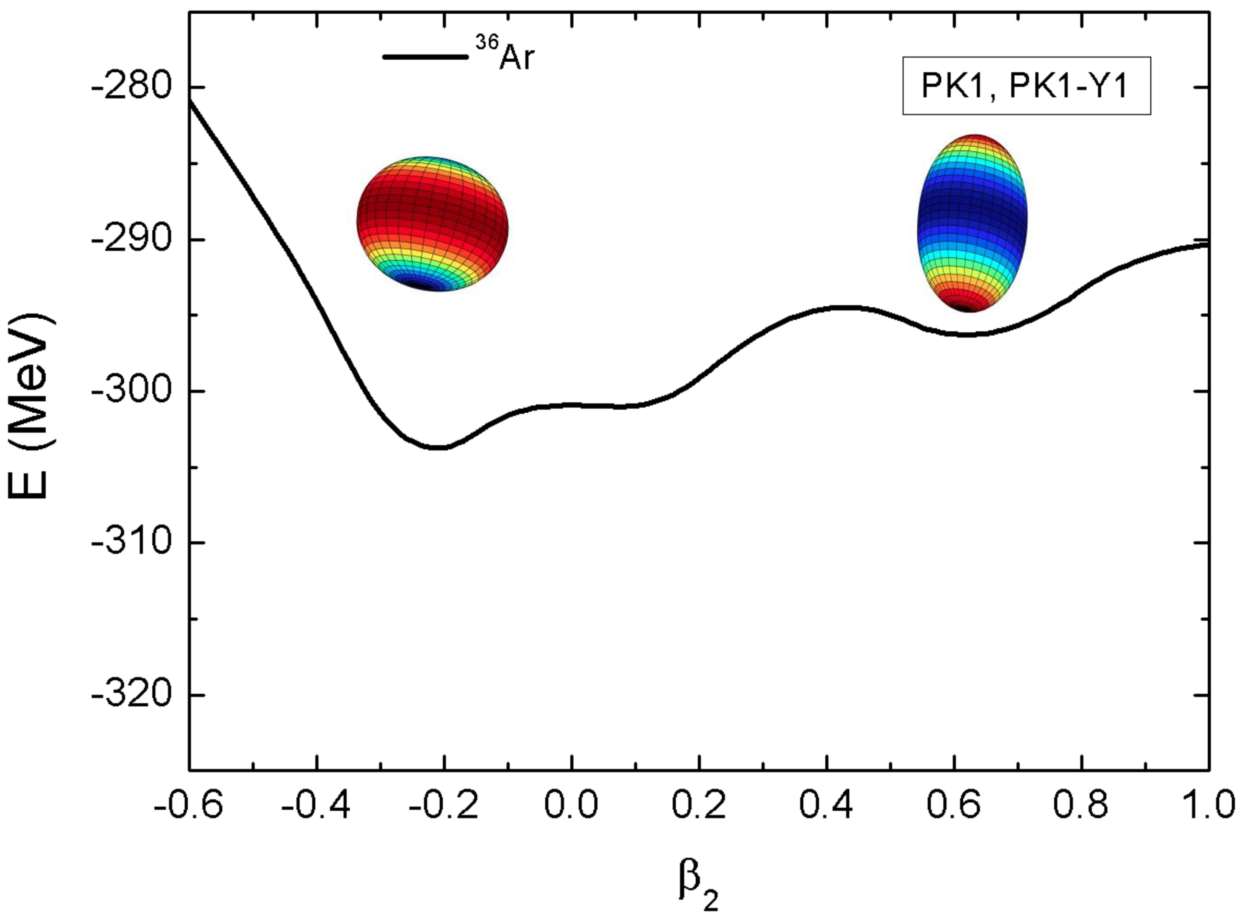

Lu_Hiyama_Sagawa_SGZ
2014_PRC89-044307

Superdeformed hypernuclei

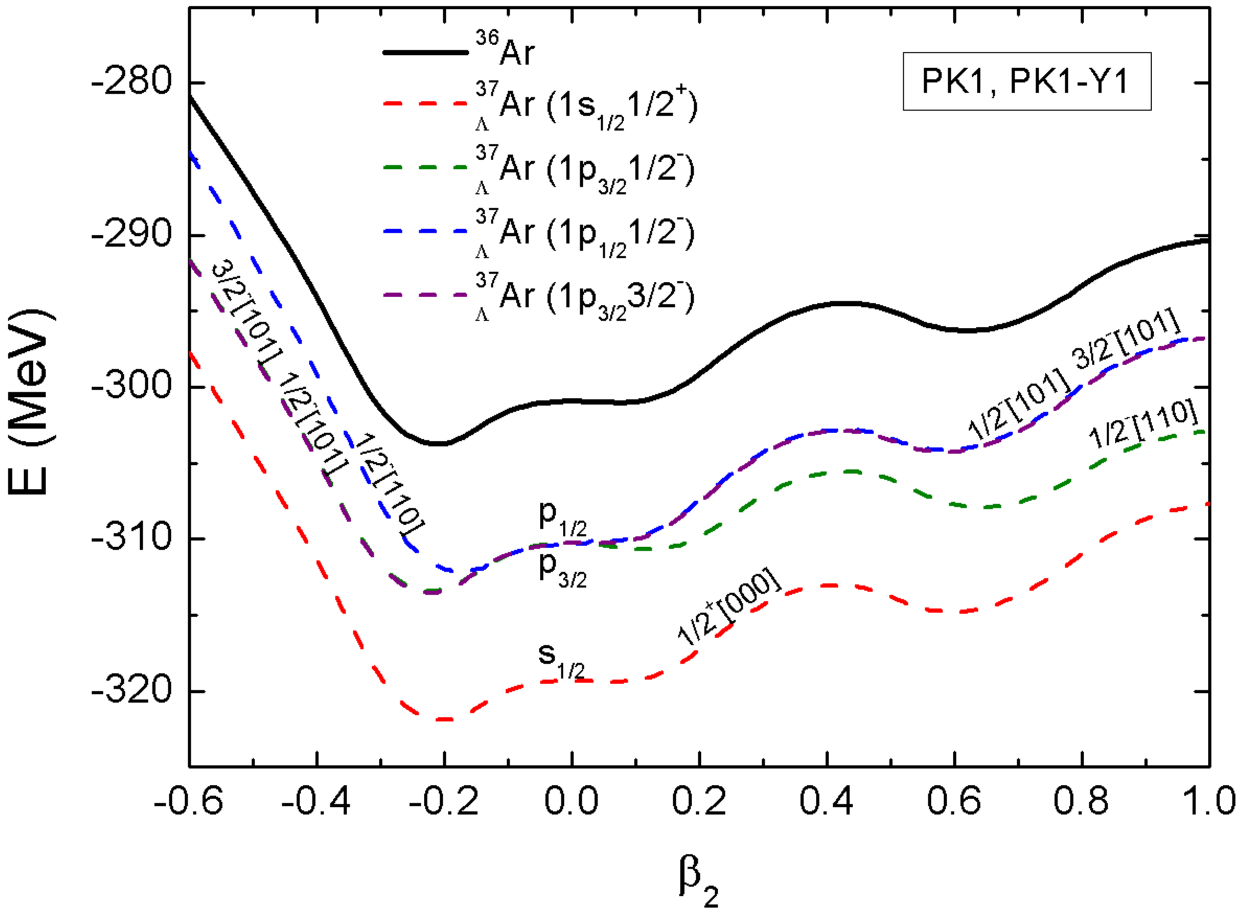

Lu_Hiyama_Sagawa_SGZ
2014_PRC89-044307

Superdeformed hypernuclei

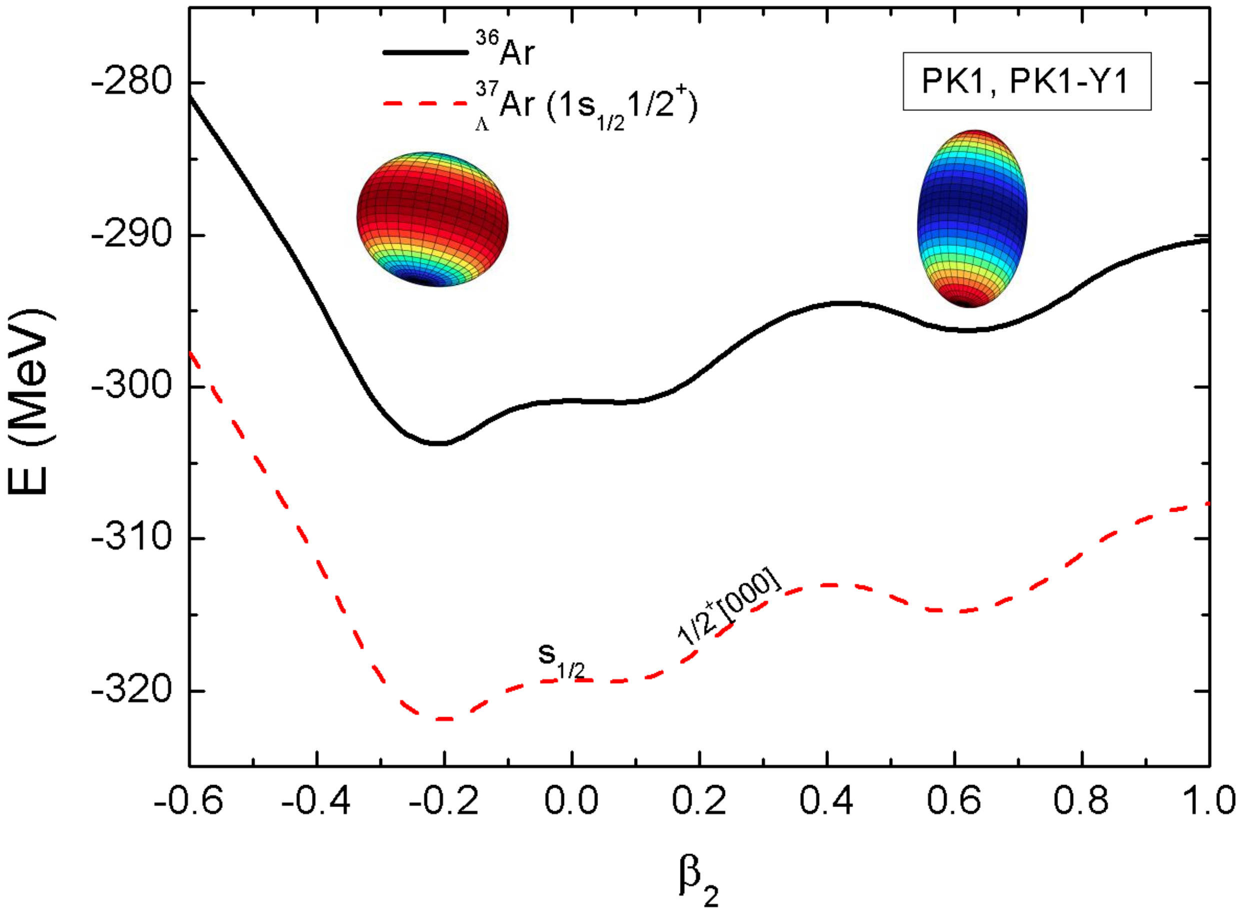

Lu_Hiyama_Sagawa_SGZ 2014_PRC89-044307

Superdeformed hypernuclei

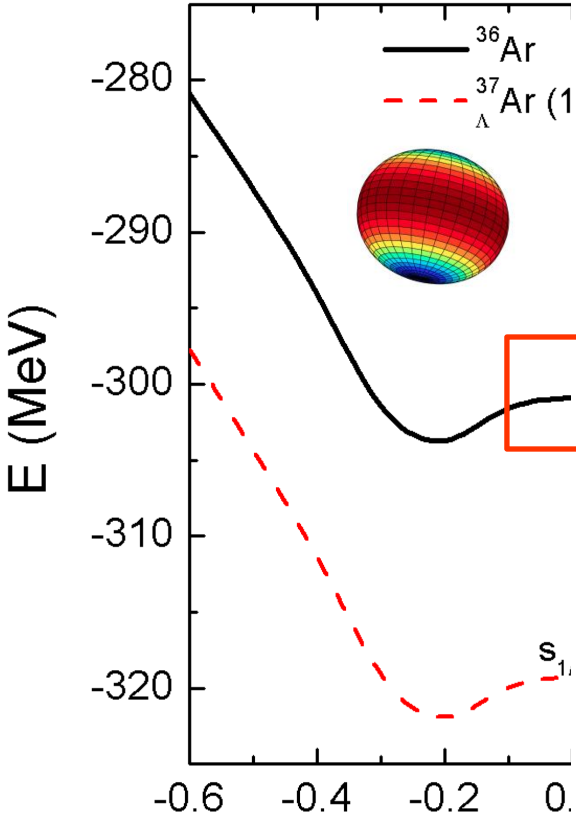

TABLE II. Calculated deformation parameter β_2, the overlap I_{overlap} defined in Eq. (11), the binding energy E, and Λ separation energy S_Λ of some Λ hypernuclei. For comparison, the binding energy of the core nucleus E_{core} is also given. The energies are in MeV.

Nucleus	β_2	I_{overlap}	E_{tot}	E_{core}	S_Λ
$^{37}_{\Lambda}$Ar	−0.204	0.1352	−321.979	−303.802	18.177
$^{37}_{\Lambda}$Ar*	0.597	0.1370	−315.194	−296.670	18.524
$^{39}_{\Lambda}$Ar	0.000	0.1360	−344.896	−326.455	18.441
$^{39}_{\Lambda}$Ar*	0.589	0.1378	−336.306	−317.448	18.858
$^{41}_{\Lambda}$Ar	−0.117	0.1357	−361.398	−342.613	18.785
$^{41}_{\Lambda}$Ar*	0.491	0.1378	−355.922	−336.852	19.070
$^{41}_{\Lambda}$Ca	0.00	0.1361	−361.422	−342.869	18.553
$^{41}_{\Lambda}$Ca*	0.70	0.1393	−350.559	−331.317	19.242
$^{33}_{\Lambda}$S	0.26	0.1376	−285.095	−267.002	18.093
$^{33}_{\Lambda}$S*	0.97	0.1243	−274.315	−257.951	16.364
$^{57}_{\Lambda}$Ni	0.00	0.1461	−506.665	−484.759	21.906
$^{57}_{\Lambda}$Ni*	0.40	0.1415	−498.610	−477.892	20.718
$^{61}_{\Lambda}$Zn	0.22	0.1438	−534.565	−512.924	21.641
$^{61}_{\Lambda}$Zn*	0.62	0.1415	−527.168	−506.238	20.930

Superdeformed hypernuclei

Lu_Hiyama_Sagawa_SGZ
2014_PRC89-044307

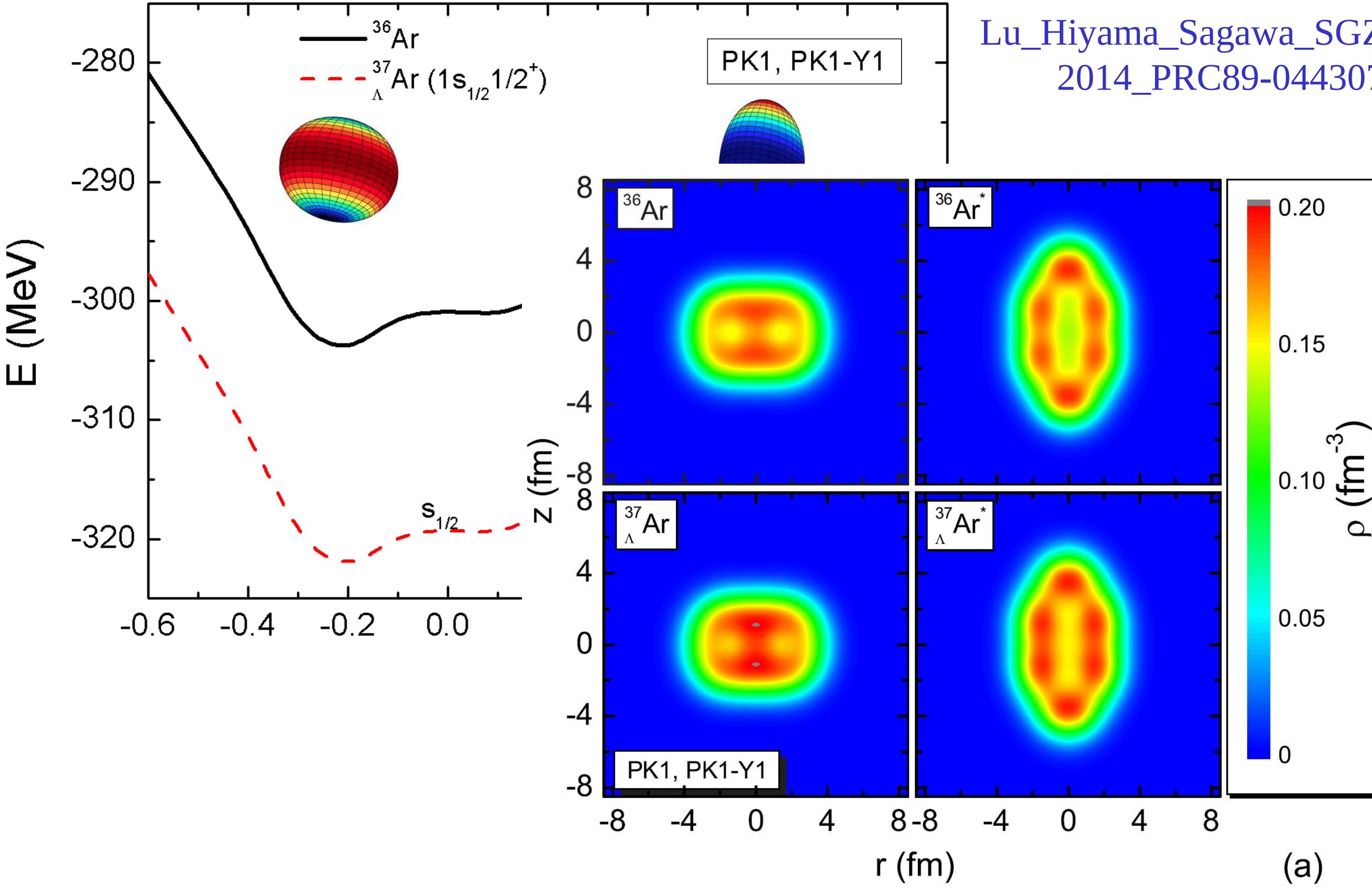

Superdeformed hypernuclei

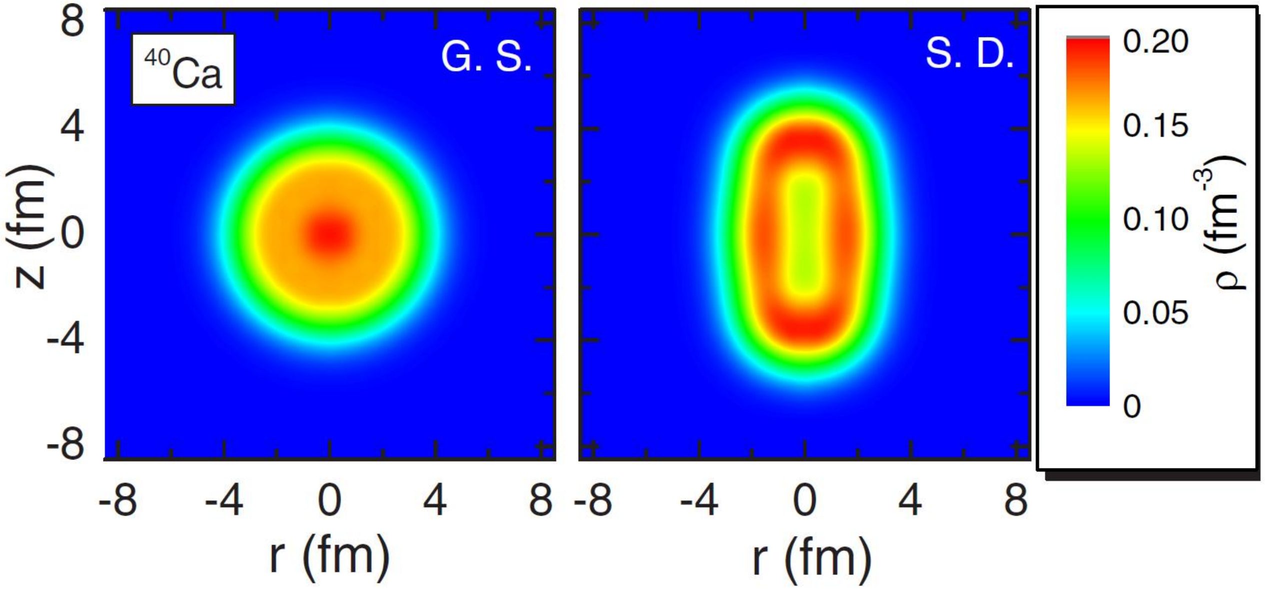

Lu_Hiyama_Sagawa_SGZ
2014_PRC89-044307

Superdeformed hypernuclei

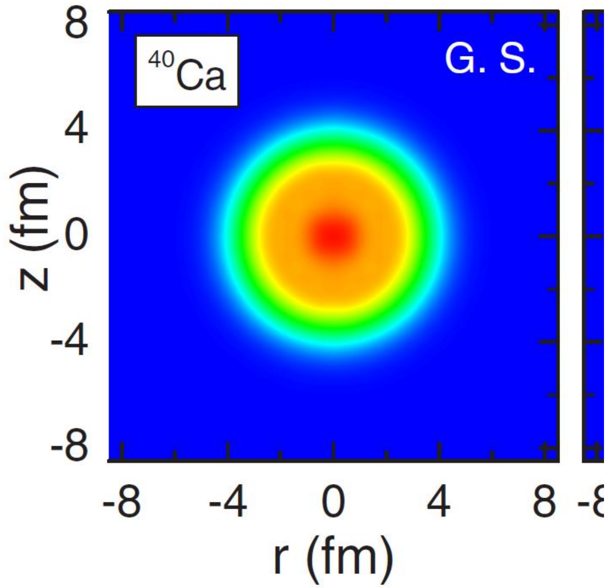

TABLE II. Calculated deformation parameter β_2, the overlap I_{overlap} defined in Eq. (11), the binding energy E, and Λ separation energy S_Λ of some Λ hypernuclei. For comparison, the binding energy of the core nucleus E_{core} is also given. The energies are in MeV.

Nucleus	β_2	I_{overlap}	E_{tot}	E_{core}	S_Λ
$^{37}_{\Lambda}$Ar	−0.204	0.1352	−321.979	−303.802	18.177
$^{37}_{\Lambda}$Ar*	0.597	0.1370	−315.194	−296.670	18.524
$^{39}_{\Lambda}$Ar	0.000	0.1360	−344.896	−326.455	18.441
$^{39}_{\Lambda}$Ar*	0.589	0.1378	−336.306	−317.448	18.858
$^{41}_{\Lambda}$Ar	−0.117	0.1357	−361.398	−342.613	18.785
$^{41}_{\Lambda}$Ar*	0.491	0.1378	−355.922	−336.852	19.070
$^{41}_{\Lambda}$Ca	0.00	0.1361	−361.422	−342.869	18.553
$^{41}_{\Lambda}$Ca*	0.70	0.1393	−350.559	−331.317	19.242
$^{33}_{\Lambda}$S	0.26	0.1376	−285.095	−267.002	18.093
$^{33}_{\Lambda}$S*	0.97	0.1243	−274.315	−257.951	16.364
$^{57}_{\Lambda}$Ni	0.00	0.1461	−506.665	−484.759	21.906
$^{57}_{\Lambda}$Ni*	0.40	0.1415	−498.610	−477.892	20.718
$^{61}_{\Lambda}$Zn	0.22	0.1438	−534.565	−512.924	21.641
$^{61}_{\Lambda}$Zn*	0.62	0.1415	−527.168	−506.238	20.930

Superdeformed hypernuclei

Isaka_Fukukawa_Kimura
Hiyama_Sagawa_Yamamoto
2014_PRC89-024310

AMD: Opposite predictions !

TABLE I. Calculated excitation energy E_x in MeV, matter quadrupole deformation β and γ (deg), and rms radii (fm). The B_Λ defined by Eq. (14) is also listed in unit of MeV for $^{41}_{\Lambda}$Ca.

	J^π	E_x (MeV)	β	γ (deg)	$r_{\rm rms}$ (fm)	B_Λ
$^{41}_{\Lambda}$Ca	$1/2^+_1$	0.00	0.10	0	3.38	19.45
	$1/2^+_2$	9.24	0.40	27	3.47	19.15
	$1/2^+_3$	11.41	0.55	13	3.58	18.01
^{40}Ca	0^+_1	0.00	0.12	12	3.39	
	0^+_2	8.94	0.40	28	3.50	
	0^+_3	9.97	0.60	17	3.63	

Superdeformed hypernuclei

LETTER

Ebran_Khan_Niksic_Vretenar 2012_Nature487-341

doi:10.1038/nature11246

How atomic nuclei cluster

J.-P. Ebran[1], E. Khan[2], T. Nikšić[3] & D. Vretenar[3]

What about
Skyrme Hartree-Fock ?

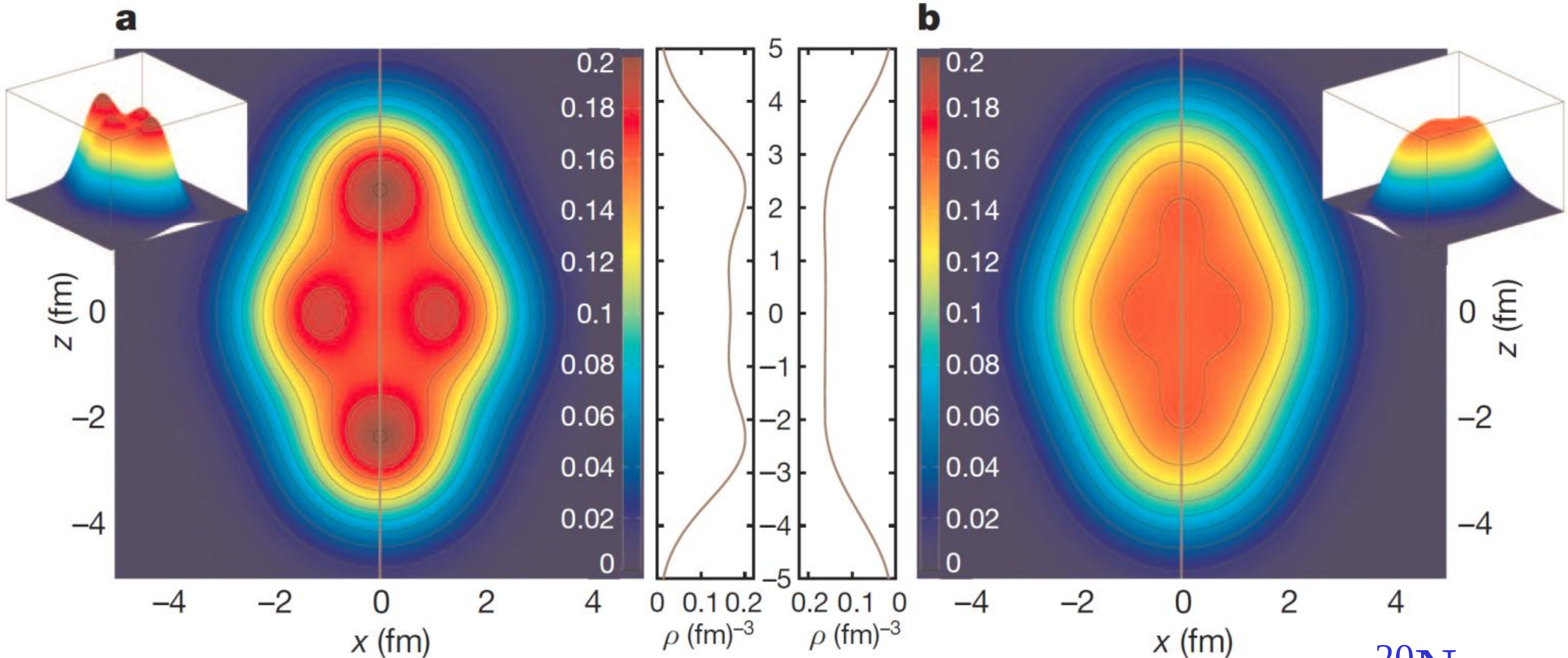

^{20}Ne

Summary

- Multidimensionally-constrained covariant density functional theories: (β_{20}, β_{22}, β_{30}, β_{32}, β_{40}, ...)
- PES & fission barriers of heavy normal nuclei
  - Triaxiality lowering systematically 2^{nd} barrier of actinides
  - Non-axial octupole correlations in N=150 isotones
  - Shallow hyperdeformed minima in actinides
- Shape of hypernuclei
  - Drastic shape changes in (^{12}C-$^{13}_{\Lambda}C$), (^{28}Si-$^{29}_{\Lambda}Si$), …
  - Localization effects in superdeformed $^{36,38,40}Ar$ & ^{40}Ca, leading to larger Λ separation energy than in ground state

Summary & perspectives

- Multidimensionally-constrained covariant density functional theories: (β_{20}, β_{22}, β_{30}, β_{32}, β_{40}, ...)
- PES & fission barriers of heavy normal nuclei
  - Triaxiality lowering systematically 2^{nd} barrier of actinides
  - Non-axial octupole correlations in *N*=150 isotones
  - Shallow hyperdeformed minima in actinides
- Shape of hypernuclei
  - Drastic shape changes in (^{12}C-$^{13}_{\Lambda}C$), (^{28}Si-$^{29}_{\Lambda}Si$), …
  - Localization effects in superdeformed $^{36,38,40}Ar$ & ^{40}Ca, leading to larger Λ separation energy than in ground state

- Systematic study of PES & B_f of superheavy nuclei
- Structure of $S=-2$ hypernuclei

Collaborators

Emiko Hiyama	RIKEN
Bing-Nan Lu (吕炳楠)	ITP/CAS & FZJ
Xu Meng (孟旭)	ITP/CAS
Hiroyuki Sagawa	RIKEN & Aizu U
Dario Vretenar	U Zagreb
En-Guang Zhao (赵恩广)	ITP/CAS
Jie Zhao (赵杰)	ITP/CAS

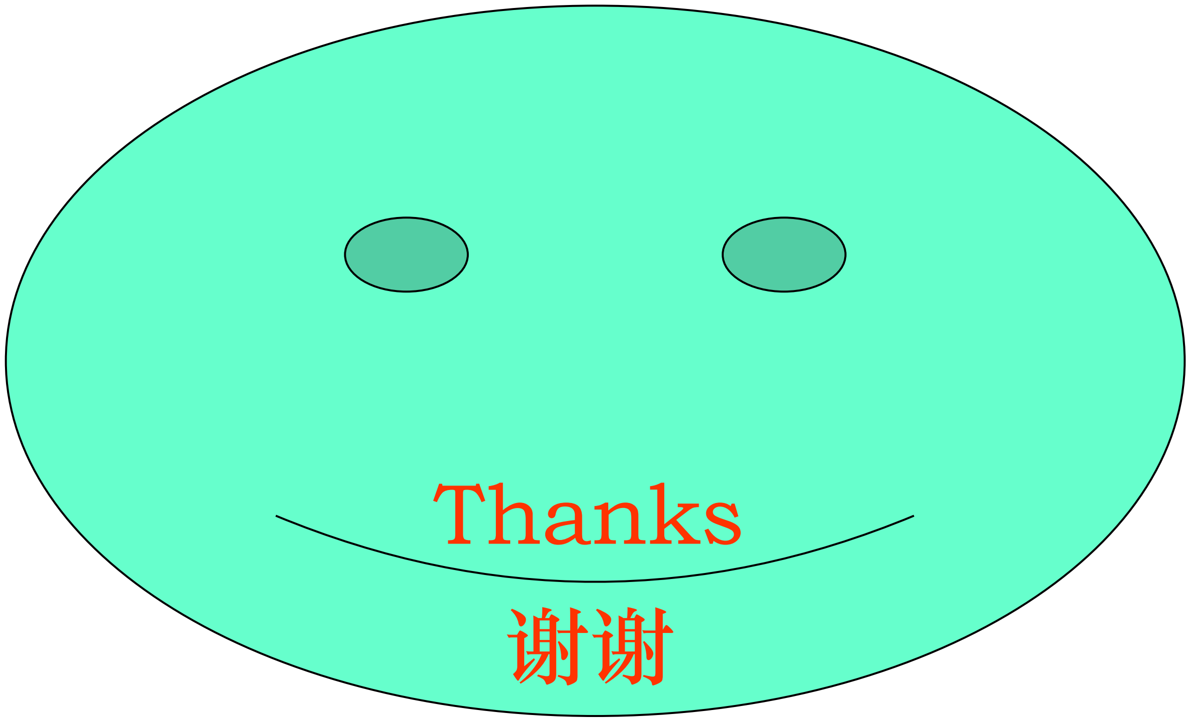

Email: sgzhou@itp.ac.cn

URL: www.itp.ac.cn/~sgzhou